



SCHOOL of
GRADUATE STUDIES
EAST TENNESSEE STATE UNIVERSITY

East Tennessee State University
**Digital Commons @ East
Tennessee State University**

Electronic Theses and Dissertations

Student Works

12-2007

Localization of a Microsporidia ADAM (A Disintegrin and Metalloprotease Domain) Protein and Identification of Potential Binding Partners.

Carrie E. Jolly

East Tennessee State University

Follow this and additional works at: <https://dc.etsu.edu/etd>

 Part of the [Amino Acids, Peptides, and Proteins Commons](#)

Recommended Citation

Jolly, Carrie E., "Localization of a Microsporidia ADAM (A Disintegrin and Metalloprotease Domain) Protein and Identification of Potential Binding Partners." (2007). *Electronic Theses and Dissertations*. Paper 2052. <https://dc.etsu.edu/etd/2052>

This Dissertation - Open Access is brought to you for free and open access by the Student Works at Digital Commons @ East Tennessee State University. It has been accepted for inclusion in Electronic Theses and Dissertations by an authorized administrator of Digital Commons @ East Tennessee State University. For more information, please contact digilib@etsu.edu.

Localization of a Microsporidia ADAM (a Disintegrin and Metalloprotease Domain) Protein
and Identification of Potential Binding Partners

A dissertation
presented to
the faculty of the Department of Microbiology
East Tennessee State University

In partial fulfillment
of the requirements for the degree
Doctor of Philosophy in Biomedical Sciences

by
Carrie E. Jolly
December 2007

J. Russell Hayman, Ph.D., Chair
Robert V. Schoborg, Ph.D.
David A. Johnson, Ph.D.
Jane E. Raulston, Ph.D.
Michelle M. Duffourc, Ph.D.
John J. Laffan, Ph.D.

Keywords: Microsporidia, *Encephalitozoon intestinalis*, *Encephalitozoon cuniculi*, ADAM,
Yeast Two-Hybrid, Polar Tube Protein

ABSTRACT

Localization of a Microsporidia ADAM (a Disintegrin and Metalloprotease Domain) Protein and Identification of Potential Binding Partners

by

Carrie E. Jolly

Microsporidia are spore-forming, obligate intracellular pathogens typically associated with opportunistic infections in immunocompromised individuals. Treatment options for microsporidia infections in humans are limited and additional research is necessary to create better therapeutic agents. For many pathogenic organisms, adhesion to the host cell surface is a prerequisite for tissue colonization and invasion. Our previous research has demonstrated a direct relationship between adherence of microsporidia spores to the surface of host cells and infectivity *in vitro*. In an effort to better understand adherence, we have turned our attention to determining what proteins may be involved in this process. Examination of the *Encephalitozoon cuniculi* genome database revealed a gene encoding a protein with sequence homology to members of the ADAM (a disintegrin and metalloprotease) family of type I transmembrane glycoproteins. The microsporidia ADAM (MADAM) protein is of interest because ADAMs are known to be involved in a variety of biological processes including cell adhesion, proteolysis, cell fusion, and signaling. The objectives for this study were to examine the localization of MADAM, analyze its potential involvement during adherence and/or host cell infection, and to identify potential binding partners or substrates. Through the use of immunoelectron transmission microscopy, we

demonstrated that MADAM is localized to the surface exposed exospore, plasma membrane, and the polar sac-anchoring disk complex (a bell-shaped structure at the spore apex involved in the infection process). Location of MADAM within the exospore and polar sac-anchoring disk suggests that MADAM is in a position to facilitate spore adherence or host cell infection. Thus far, we have been unable to conclusively demonstrate that MADAM is involved in either event. Through the use of a yeast two-hybrid system, we were able to identify polar tube protein 3 (PTP3) as a potential binding partner or substrate for the MADAM protein. The interaction between MADAM and PTP3 was confirmed by *in vitro* co-immunoprecipitation. PTP3 is hypothesized to be involved in the process of polar tube extrusion by stabilizing the interaction between PTP1-PTP2 polymers. Further analysis of the interaction between MADAM and PTP3 may lead to a better understanding of the events that occur during polar tube extrusion.

DEDICATION

I would like to dedicate this manuscript to my daughter, Brooklyn Elise Boster. I often wonder how we have both managed to survive the past ten years physically and emotionally intact. I hope that one day you can look back on this journey and understand the importance of what we were able to accomplish.

ACKNOWLEDGMENTS

I would like to recognize some of the individuals who were instrumental in my development along this journey. To everyone who offered support, encouragement, and faith—thank you. I know that even when I doubted myself, you never did. To everyone who questioned and challenged my abilities—thank you. Because of you, I learned how to persevere.

CONTENTS

	Page
ABSTRACT	2
DEDICATION	4
ACKNOWLEDGEMENTS	5
LIST OF TABLES	8
LIST OF FIGURES	9
Chapter	
1. INTRODUCTION	12
Microsporidia Infection in Humans.....	12
Microsporidia Spore Structure and Development	14
Microsporidia Spore Activation and Polar Tube Discharge.....	16
Microsporidia Spore Adherence to the Host Cell Surface.....	18
The Microsporidia ADAM Protein	20
Specific Aims	25
2. MATERIALS AND METHODS	26
Microsporidia Spore Propagation and Purification.....	26
Cloning and Recombinant Expression of the <i>E. cuniculi</i> MADAM Protein	26
Purification of the Histidine-Tagged Recombinant MADAM Protein and Antibody Production	27
Western Analysis of <i>E. cuniculi</i> and <i>E. intestinalis</i> Spore Protein	28
Identification of the ~143kDa <i>E. cuniculi</i> Spore Protein	28
Immunolabeling and Transmission Electron Microscopy.....	29
Cloning, Recombinant Expression, and Purification of <i>E. cuniculi</i> MADAM Deletion Mutants	30
Spore Adherence Assays.....	31

Host Cell Infectivity Assays	32
Yeast Two-Hybrid Analysis	33
Construction of GAL4 DNA-BD+MADAM Fusion Vectors	34
Transformation of Yeast with the GAL4 DNA-BD+MADAM Fusion Vectors.....	38
Generation of the cDNA Library from <i>E. intestinalis</i> -Infected Vero Host Cells	38
Construction of the GAL4 AD+cDNA Library Fusion Vectors	41
Analysis of Positive Yeast Two-Hybrid Interactions.....	43
Construction of the GAL4 AD+Polar Tube Protein 1, 2, and 3 Fusion Vectors	45
<i>In Vitro</i> Transcription, Translation, and Co-Immunoprecipitation	48
3. RESULTS	50
Recombinant Expression of MADAM Protein for Polyclonal Antibody Production	50
Western Analysis of MADAM Protein from <i>E. cuniculi</i> and <i>E. intestinalis</i>	51
Identification of the ~143kDa Protein Recognized by the Anti-rMADAM-His-Tag Antibodies	52
Localization of the MADAM Protein within <i>E. cuniculi</i> and <i>E. intestinalis</i>	55
Spore Adherence and Host Cell Infectivity Assays.....	60
Identification of Potential Protein-Protein Interactions Involving MADAM	62
Confirmation of Yeast Two-Hybrid Interactions Using <i>In Vitro</i> Co-Immunoprecipitation	80
4. CONCLUSIONS	81
REFERENCES	91
VITA	95

LIST OF TABLES

Table		Page
1.	Primers Used to Generate MADAM PCR Products for Insertion into the pGBKT7 Vector	37
2.	Primers Used to Generate <i>E. cuniculi</i> and <i>E. intestinalis</i> Polar Tube Protein PCR Products for Insertion into the pGADT7-Rec Vector	47
3.	Basic Local Alignment Tool (BLAST) Identification of PCR Amplified cDNA Inserts from Yeast Colonies Demonstrating Potential Interactions Involving the MADAM (Δ SS/ Δ TM) Protein	66
4.	Proteins Commonly Identified as False-Positives During Yeast Two-Hybrid Analysis	72

LIST OF FIGURES

Figure		Page
1.	Ultrastructure of <i>Encephalitozoon intestinalis</i> within Vero E6 Host Cells	15
2.	Phases of Polar Tube Discharge in <i>Encephalitozoon hellem</i>	17
3.	Effect of Inhibition of <i>E. intestinalis</i> Spore Adherence on Host Cell Infection.....	19
4.	Predicted MADAM Domain Structure Compared to the Consensus ADAM Domains.....	21
5.	Global Pairwise Alignment of Metalloprotease Active Site Sequences from MADAM and Several Other ADAM Family Members.....	23
6.	Global Pairwise Alignment of Disintegrin Domain Sequences from MADAM and Several Other ADAM Family Members	24
7.	Diagram of Yeast Two-Hybrid Analysis.....	34
8.	Diagram of the pGBKT7 Vector.....	36
9.	MADAM Constructs Used for Yeast Two-Hybrid Analysis.....	37
10.	Synthesis of ds cDNA Using the SMART™ Technology.....	40
11.	Diagram of the pGADT7-Rec Vector.....	42
12.	Homologous Recombination of ds cDNA and the pGADT7-Rec Vector.....	43
13.	Overview of <i>In Vitro</i> Transcription, Translation, and Co-Immunoprecipitation	49
14.	Expression of rMADAM-His-Tag Protein	50
15.	Western Analysis of MADAM Protein	51

16.	Purification and Identification of the ~143kDa <i>E. cuniculi</i> Protein.....	53
17.	Western Analysis of <i>E. cuniculi</i> and <i>E. intestinalis</i> Protein Using the Rabbit Pre-Immune Serum.....	54
18.	Immunolabeling of <i>E. intestinalis</i> -Infected RK-13 Cells Using Antibodies from the Pre-Immune Serum.....	55
19.	Localization of MADAM within <i>E. cuniculi</i>	57
20.	Localization of MADAM within <i>E. intestinalis</i>	58
21.	Localization of MADAM within Various Stages of <i>E. intestinalis</i> Development.....	59
22.	MADAM Constructs Introduced into the pET-21a Vector	60
23.	Analysis of Spore Adherence in the Presence of Recombinant MADAM Proteins.....	61
24.	Analysis of Host Cell Infection in the Presence of Recombinant MADAM Proteins.....	62
25.	Amplification of cDNA Inserts from Potential Positive Yeast Clones.....	65
26.	Chromatogram Demonstrating an Unreadable DNA Sequence	70
27.	Localization of PTP3 within <i>E. cuniculi</i>	74
28.	Yeast Two-Hybrid Analysis of GAL4 DNA-BD+MADAM (Δ SS/ Δ TM) and GAL4 AD+ <i>E. cuniculi</i> Polar Tube Protein 1, 2, and 3.....	77
29.	Yeast Two-Hybrid Analysis of MADAM and the <i>E. cuniculi</i> Polar Tube Proteins.....	78
30.	Yeast Two-Hybrid Analysis of MADAM and the <i>E. intestinalis</i> Polar Tube Proteins.....	79
31.	<i>In Vitro</i> Co-Immunoprecipitation Studies Involving MADAM, EcPTP2, and	

CHAPTER 1

INTRODUCTION

Microsporidia Infection in Humans

Microsporidia are spore-forming, obligate intracellular, fungal-related pathogens with a diverse host range that includes most vertebrates and invertebrates. Traditionally, microsporidiosis was considered an economically devastating disease of insects (silkworm and honeybee), fish, and fur-bearing mammals (mink, laboratory rabbits, and rodents) (Didier and others 2004). Today, microsporidia are recognized as an emerging and opportunistic pathogen of humans, particularly those infected with the human immunodeficiency virus (HIV) (Didier and Weiss 2006). In addition to individuals with HIV, microsporidia infections have been documented in an assortment of human populations including travelers, contact lens wearers, malnourished children, organ transplant recipients, and the elderly (Deplazes and others 2000; Didier and others 2004).

Only 14 of the estimated 1,200 species of microsporidia are known to infect humans (Didier and others 2004). *Enterocytozoon bieneusi* and *Encephalitozoon intestinalis* are the most frequently diagnosed causes of human microsporidiosis (Mathis and others 2005). Most cases of microsporidia infection are thought to occur through ingestion of the environmentally stable spores, which results in a primary infection of the small intestine epithelium (Didier and Weiss 2006). Exact sources of microsporidia infection in humans and possible routes of transmission remain largely undetermined. However, microsporidia known to infect humans have been identified in domestic and wild animals, which supports the hypothesis that microsporidiosis is a zoonotic disease (Didier and Weiss 2006).

The most common clinical manifestations of microsporidiosis are self-limiting diarrhea in immunocompetent individuals and severe persistent diarrhea in the immunocompromised (Didier and others 2004). Severe, persistent diarrhea in immunocompromised individuals is often accompanied by fever, appetite loss, weight loss, and wasting syndrome (Didier and others 2004). *Encephalitozoon* species cause disseminated infections with a number of serious clinical manifestations including myositis, encephalitis, sinusitis, pneumonia, hepatitis, and peritonitis (Didier and Weiss 2006). The clinical manifestations of microsporidia infection are determined by a number of factors including immune status of the host, the location of infection, and which species is responsible for the infection.

Human microsporidial infections are most often treated with either albendazole or fumagillin (Didier and Weiss 2006). Albendazole, an anti-mitotic agent due to its ability to disrupt tubulin polymerization, stops mitosis in both the microsporidia and the host cell (Conteas and others 2000). Short-term albendazole therapy does not result in clearance of the infection but rather prevents the microsporidia from spreading. Although albendazole is successful at treating microsporidiosis due to *Encephalitozoon* species, it is not an effective treatment against the most common cause of human microsporidiosis, *Enterocytozoon bieneusi* (Conteas and others 2000). Fumagillin, an antibiotic produced by the fungus *Aspergillus fumigatus*, selectively inhibits the activity of methionine aminopeptidase 2 (MetAP2) from the host cell and developing microsporidia (Upadhyay and others 2006). Fumagillin can be used to successfully treat gastrointestinal infections attributed to *Enterocytozoon bieneusi* as well as ocular infections due to *Encephalitozoon* species (Conteas and others 2000). Unfortunately, patients often develop thrombocytopenia and neutropenia that resolve after cessation of fumagillin therapy (Conteas and others 2000).

Treatment options for microsporidia infections in humans are limited and additional research is necessary to create better therapeutic agents or to manage the side effects of current treatments.

Microsporidia Spore Structure and Development

Mature spores are the environmentally resistant, infectious stage of microsporidial development (Bigliardi and Sacchi 2001). Environmental stability is provided by a rigid spore wall that consists of an outer electron-dense exospore composed of proteinaceous material, an electron-lucent endospore composed of protein and chitin or a chitin-like material, and an inner plasma membrane (Bigliardi and Sacchi 2001). Mature microsporidia spores contain several characteristic structures including a lamellar polaroplast, posterior vacuole, anchoring disk, and an organelle unique to the phylum *Microspora* called the polar filament or polar tube (Figure 1). The polar tube arises from an anchoring disk in the anterior region then coils around the infectious sporoplasm in the posterior region of the mature spore. Microsporidia are considered eukaryotes mainly because they possess a nucleus but also resemble prokaryotic organisms as they lack mitochondria, peroxisomes, and a typical Golgi apparatus (Bigliardi and Sacchi 2001).

As stated previously, the majority of microsporidia infections are thought to occur via ingestion of the environmentally stable spores, which results in a primary infection of the small intestine epithelium. Traditionally, microsporidia were believed to infect a host cell by extruding the polar tube at a velocity fast enough to pierce the host cell plasma membrane thereby allowing the infectious sporoplasm to pass through the hollow polar tube and into the host cell cytoplasm (Vivares and Metenier 2001). Once within the host cell cytoplasm, the infectious sporoplasm undergoes a phase of proliferative growth by nuclear division

known as merogony (Bigliardi and Sacchi 2001). Meronts, which consist of a simple plasma membrane and sparse organelles, transition into sporonts that are characterized by the appearance of an electron-dense material along the outer membrane (Figure 1). Sporonts mature into sporoblasts following additional development of the organelles. Sporoblasts are the final phase before the appearance of mature spores with fully formed and properly oriented organelles (Figure 1).

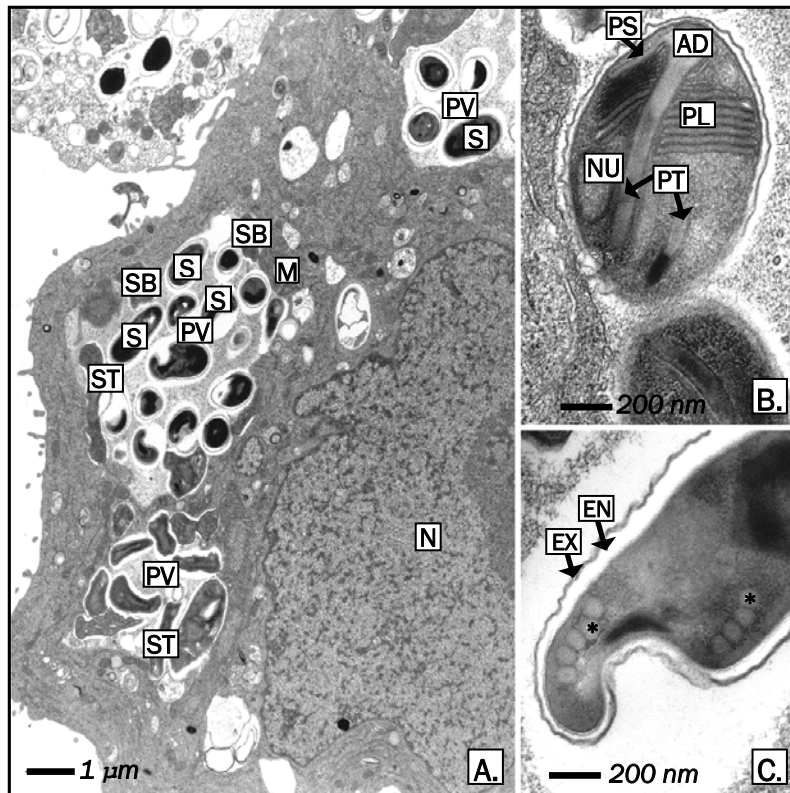


Figure 1 Ultrastructure of *Encephalitozoon intestinalis* within Vero E6 host cells. (A) Mature *E. intestinalis* spores (S) and other developmental stages including meronts (M), sporonts (ST), and sporoblasts (SB) are observed developing within several parasitophorous vacuoles (PV). Note the host cell nucleus (N) compressed to the periphery. (B) Structures within the mature spore include the nucleus (NU), lamellar polaroplast (PL), polar tube (PT), polar sac (PS), and an anchoring disc (AD). (C) A mature *E. intestinalis* spore demonstrating the electron-dense exospore (EX), an inner electron-lucent endospore (EN), and the polar tube with 4 or 5 coils (*) around the posterior region. (adapted from Croppo and others 1998).

Each stage of microsporidia development can be observed simultaneously within an infected host cell (Figure 1). *Encephalitozoon* species are segregated within a compartment known as the parasitophorous vacuole while other species such as *Enterocytozoon bieneusi* develop in direct contact with the host cell cytoplasm. A host cell will support microsporidia development for several days before rupture of the host cell plasma membrane and the parasitophorous vacuole resulting in the release of mature spores into the extracellular environment. Exactly how a host cell can support microsporidia development without apparent detriment for several days remains to be determined. It has been suggested that microsporidia manipulate the host cell cycle and/or apoptotic pathways during development (Scanlon and others 2000; del Aguila and others 2006).

Microsporidia Spore Activation and Polar Tube Discharge

Although many of the details regarding how polar tube extrusion leads to host cell infection are still undetermined, the following series of events are thought to be involved: 1) activation of the spore, 2) increase in internal osmotic pressure, 3) discharge of the polar tube, and 4) passage of the infectious sporoplasm through the polar tube and into the host cell cytoplasm (Xu and Weiss 2005). Numerous stimuli have been reported to induce polar tube discharge including changes in pH, addition of various cations and anions, dehydration followed by rehydration, and hydrogen peroxide (Xu and Weiss 2005). Each stimulus studied thus far appears to elicit an increase in osmotic pressure inside the spore followed by an influx of water and swelling of the polaroplast (Bigliardi and Sacchi 2001).

As the polaroplast swells, the anchoring disk protrudes to form a collar-like structure that serves to hold the polar tube in place during discharge (Figure 2). As the polar tube emerges from the spore apex, it is thought to either 1) exit at a high velocity allowing it to

pierce the host cell plasma membrane like a hypodermic needle or 2) enters the host cell by a phagocytic process brought about by an interaction between the spore apex and the host cell surface (Xu and Weiss 2005). As the posterior vacuole begins to swell, pressure forces the infectious sporoplasm through the polar tube into the host cell cytoplasm (Bigliardi and Sacchi 2001).

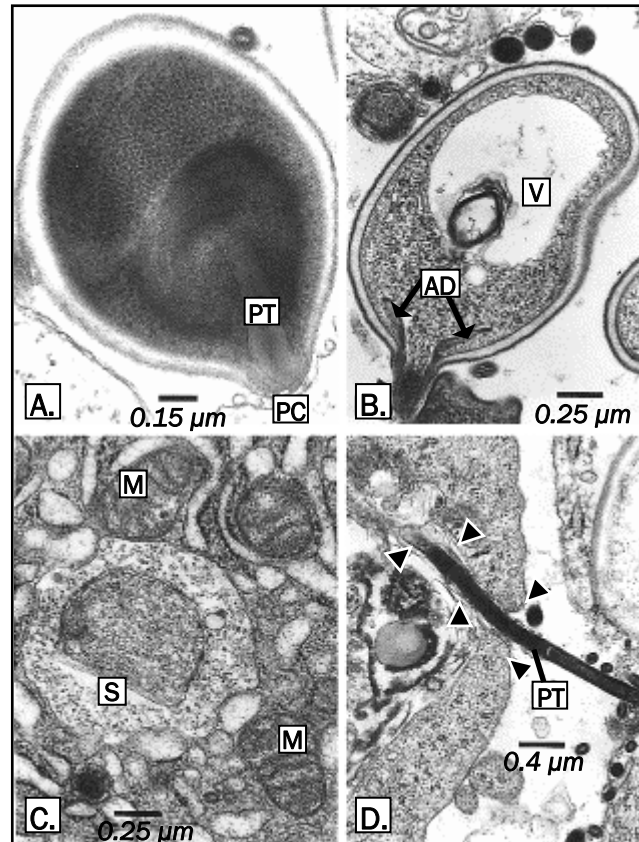


Figure 2 Phases of polar tube discharge in *Encephalitozoon hellem*. (A) At the beginning of polar tube discharge, the polar tube (PT) protrudes from the spore apex at the polar cap (PC) or anchoring disk region. (B) As polar tube discharge continues, the anchoring disk (AD) forms a collar-like structure and the posterior vacuole (V) enlarges in order to force the infectious sporoplasm through the polar tube. (C) Once inside the host cell cytoplasm, the infectious sporoplasm (S) can be seen surrounded by host cell mitochondria (M). (D) In this electron micrograph, the polar tube (PT) appears to be enclosed within an invagination of the host cell membrane (arrow heads). (adapted from Bigliardi and Sacchi 2001).

Microsporidia Spore Adherence to the Host Cell Surface

Adhesion to the host cell surface is a prerequisite to tissue colonization and invasion for many pathogenic organisms. During *in vitro* propagation, microsporidia spores can be observed adhering to host cells and routine washing does not remove these attached spores (Hayman and others 2005). We hypothesize that adherence of microsporidia spores to the host cell surface is an event that may trigger polar tube extrusion and subsequent host cell infection. Numerous organisms including bacteria, viruses, and parasites exploit host cell glycosaminoglycans as adhesion receptors (Rostand and Esko 1997). In fact, we have demonstrated that in an *in vitro* system *E. intestinalis* spores adhere to the host cell surface through at least one mechanism involving sulfated glycosaminoglycans (Hayman and others 2005).

Glycosaminoglycans are unbranched polysaccharide chains linked to transmembrane proteins expressed on the surface of nearly all mammalian cells (Hallak and others 2000). Some glycosaminoglycans, including heparin sulfate and chondroitin sulfate A (CSA), are sulfated and therefore possess an overall negative charge (Hallak and others 2000). We found that addition of sulfated glycosaminoglycans, like CSA, to the tissue culture medium results in a decrease in *E. intestinalis* spore adherence to the host cell surface and a decrease in the percentage of infected host cells (Figure 3) (Hayman and others 2005). A separate group of researchers found similar results during their investigation of *E. intestinalis* spore phagocytosis by differentiated intestinal epithelial cells (Leitch and others 2005).

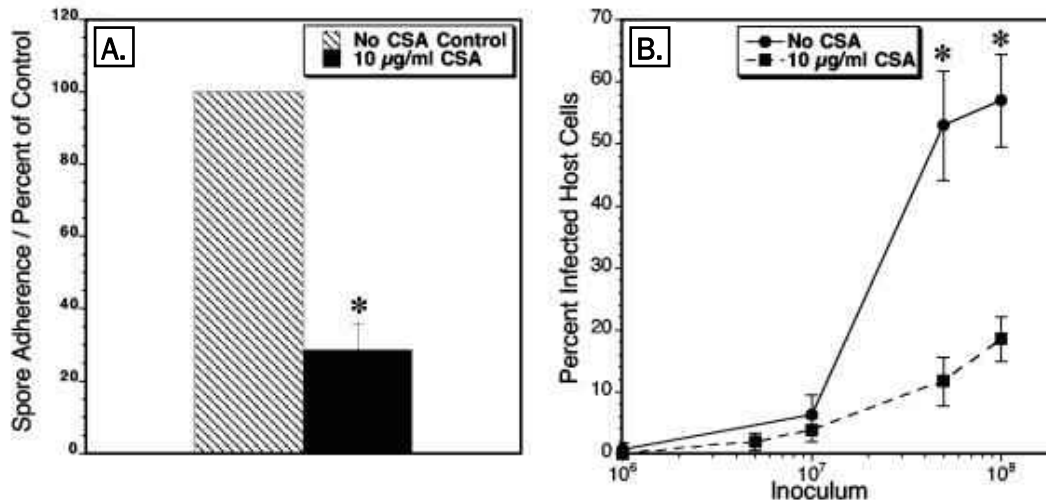


Figure 3 Effect of inhibition of *E. intestinalis* spore adherence on host cell infection. Vero host cell monolayers were incubated with *E. intestinalis* spores in the presence or absence of chondroitin sulfate A (CSA). Following an incubation period, each coverslip was washed to remove unbound spores. One set of coverslips were processed to determine the amount of adherence inhibition (A) while the remaining coverslips were returned to culture for later analysis of infected host cells (B). Addition of CSA to the tissue culture medium resulted in a 72% decrease in *E. intestinalis* spore adherence as compared to the control (A) and a 68-78% decrease in infectivity depending on the quantity of *E. intestinalis* spores (B). (adapted from Hayman and others 2005).

To further characterize the factors involved in microsporidia adherence the role of divalent cations was examined. Divalent cations are known effectors of numerous host-pathogen interactions (Anzinger and others 2006; Southern and others 2006). Addition of exogenous manganese and magnesium to the tissue culture medium resulted in an increase in adherence of microsporidia spores to the host cell monolayer and a subsequent increase in host cell infection (Southern and others 2006). Interestingly, calcium did not contribute to an increase in microsporidia adherence but did lead to an increase in host cell infection (Southern and others 2006). Calcium, which is known to play a role in the swelling of the polaroplast during polar tube extrusion, is hypothesized to actually increase the occurrence of polar tube extrusion and subsequent host cell infection in our *in vitro* system. In the

presence of chelating agents, we were able to eliminate the augmentation of microsporidia spore adherence and host cell infection by the divalent cations (Southern and others 2006).

Like many other pathogenic intracellular organisms, microsporidia appear to use adherence to the host cell surface as a mechanism to facilitate invasion. In an effort to better understand the mechanism of microsporidia spore adherence, we have turned our attention to determining what microsporidia proteins may be involved in this process. Identification of microsporidia ligands and host cell receptors that mediate adherence of the spore to the host cell surface may lead to the development of novel therapies aimed at preventing infection.

The Microsporidia ADAM Protein

To identify microsporidia proteins potentially involved in adherence, the *Encephalitozoon cuniculi* genome database was searched for genes that encode proteins with recognizable adhesion domains. This examination revealed a protein (CAD25398) with sequence homology to members of the ADAM (a disintegrin and metalloprotease domain) family. ADAMs have been described in a diverse group of organisms including mammals (i.e. *Homo sapiens* and *Mus musculus*), insects (i.e. *Drosophila* and *Apis*), purple sea urchins (*Strongylocentrotus purpuratus*), frogs (*Xenopus*), and fungi (*S. pombe*) (Rise and Burke 2002). ADAMs are a group of type I transmembrane glycoproteins involved in a variety of biological processes including cell adhesion, proteolysis, cell fusion, and signaling (White 2003). For example, ADAM10 has been implicated in the process of tumor cell metastasis through at least one mechanism involving cleavage of the cellular adhesion molecule, E-cadherin (Reiss and others 2006). Initial studies on the potential role of ADAMs in pathogenesis of human disease has revealed an association of several ADAMs with

diseases such as rheumatoid arthritis, Crohn's disease, diabetes, Alzheimer's, cancer, asthma, and microbial infections (Tousseyn and others 2006).

The theoretical molecular weight and isoelectric point of this microsporidia ADAM protein (MADAM) are predicted to be 61kDa and 5.80, respectively. Analysis of MADAM using the Conserved Domain Database revealed motifs in the sequence similar to those found in the snake venom disintegrins (E-value = $4e^{-13}$) and zinc-dependent metalloproteases (E-value = $1e^{-5}$), which includes the ADAM family (Marchler-Bauer and Bryant 2004). Most ADAMs share a common multi-domain organization consisting of a signal sequence, a pro-domain, a metalloprotease domain, a disintegrin-like domain, a cysteine-rich domain, an epidermal growth factor (EGF)-like domain, and a transmembrane domain followed by a cytoplasmic tail (White 2003). Like other ADAMs, MADAM has a predicted signal sequence, pro-domain, metalloprotease domain, disintegrin-like domain, and a transmembrane domain (Figure 4). In contrast to other ADAMs, MADAM lacks a recognizable cysteine-rich domain, an EGF-like domain, and a cytoplasmic tail but does have a region without homology to any identified proteins located between the disintegrin and transmembrane domains (Figure 4).

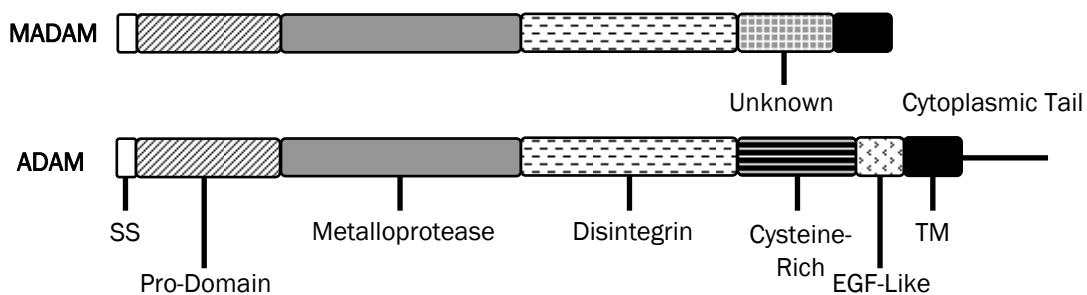


Figure 4 Predicted MADAM domain structure compared to the consensus ADAM domains. MADAM lacks a predicted cysteine-rich domain, an EGF-like domain, and a cytoplasmic tail but instead possesses a region of unknown homology between the disintegrin and transmembrane domains.

The N-terminal region consists of a signal sequence that is responsible for directing ADAMs into the secretory pathway and the pro-domain that functions in maturation of the protein (Seals and Courtneidge 2003). In many cases, the pro-domain maintains the metalloprotease domain in an inactive conformation by using what is known as a cysteine-switch mechanism (Tousseyn and others 2006). In the cysteine-switch mechanism, an unpaired cysteine residue located in the pro-domain preferentially coordinates the zinc atom required within the zinc-dependent catalytic site of the metalloprotease domain (Seals and Courtneidge 2003). While several ADAMs contain an odd number of cysteine residues within their sequence, MADAM contains an even number of closely spaced cysteine residues which suggests that MADAM may not use the cysteine-switch mechanism. In order for the metalloprotease domain to become active, a conformational change must occur by proteolytic or autocatalytic removal of the pro-domain. Furin, a pro-protein convertase, is known to cleave the pro-domain of ADAMs at the conserved recognition sequence, Rx(R/K)R (Tousseyn and others 2006). MADAM does not have a recognizable pro-protein convertase recognition sequence within its pro-domain. Therefore, MADAM pro-domain removal may occur through cleavage by an unidentified microsporidia or host protease or by an autocatalytic mechanism as is the case for ADAM8 and ADAM28 (Seals and Courtneidge 2003).

MADAM is predicted to belong to a large superfamily of proteases known as the metzincin family, which includes ADAM, ADAMTS, BMP1/TLL, meprin, and matrix metalloproteases (Huxley-Jones and others 2007). Members of the metzincin superfamily are characterized by the presence of a conserved zinc-dependent catalytic site sequence as well as a conserved methionine residue known as the 'Met-Turn', which appears to be essential in maintaining integrity of the zinc binding site (Stocker and others 1995). Of the

38+ known ADAM proteins, at least 26 contain the conserved zinc-dependent catalytic site sequence (HExxHxxGxxH) within their metalloprotease domain and are predicted to be catalytically active (White 2003) and (http://www.people.virginia.edu/~jw7g/Table_of_the_ADAMs.html). Based on global pairwise alignment, MADAM does appear to possess the conserved zinc-dependent catalytic site sequence and a 'Met-Turn' (Figure 5).

```

MADAM      (304) - VLAHEIAHALGAEH EE -GGR-----CLMRE - (328)
ADAM - 9   (344) - IVAHELGHNLGMNHDD -GRDCSCGAK-----SCIMNS - (375)
ADAM - 12  (347) - TLAHELGHNF GMNHDTLDRGCSCQMA-----VEKGGCIMNA - (383)
ADAM - 10  (380) - TFAHEVGHNF GSPHDS -GTECTPGESKNLGQKENGN YIMYA - (420)
ADAM - 17  (402) - VTTHELGHNF GAEHDP -DGLAE CAPNED-----QGGKYVMYP - (438)
--HExxHxxGxxH--                               --CIM--

```

Figure 5 Global pairwise alignment of metalloprotease active site sequences from MADAM and several other ADAM family members. The metalloprotease active site from MADAM contains the conserved zinc-dependent catalytic site sequence (HExxHxxGxxH) and 'Met-Turn' (CIM) that are indicative of metallo-proteases from the metzincin family. Like other ADAMs that possess this conserved metallo-protease domain, MADAM is predicted to be catalytically active.

Disintegrin domains were originally described as the component of snake venom metalloproteases responsible for preventing platelet aggregation by binding to platelet integrins (Seals and Courtneidge 2003). Many of the snake venom metalloproteases have an RGD consensus motif within their disintegrin domain that mediates binding to integrins (Seals and Courtneidge 2003). Of the 38+ known ADAMs, human ADAM15 is the only one that has an RGD sequence in the disintegrin domain (Seals and Courtneidge 2003). Several other ADAMs, excluding ADAM10 and ADAM17, bind the integrin $\alpha_9\beta_1$ via a conserved sequence, Rx6DLPEF, located in the disintegrin domain (Eto and others 2002). Global pairwise alignment of the MADAM disintegrin domain with other ADAMs demonstrates that sequence identities range from 33% for ADAM10 to 41% for ADAM9. This high level of identity is due in part to the presence of 14 conserved cysteine residues within the MADAM

disintegrin domain, which suggests that MADAM may have a secondary structure and function similar to other ADAMs (Figure 6). Interestingly, MADAM contains a five amino acid insertion, NIHKM, within the area considered to be the integrin-binding region of the disintegrin domain (Figure 6).

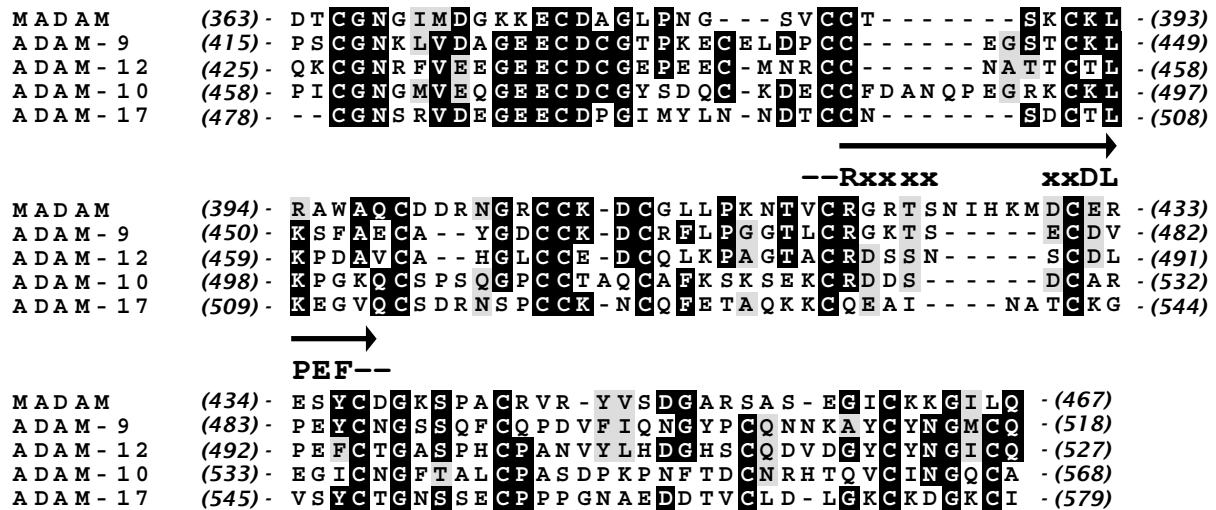


Figure 6 Global pairwise alignment of disintegrin domain sequences from MADAM and several other ADAM family members. MADAM has high sequence similarity to other ADAMs due in part to conservation of several cysteine residues. The region responsible for integrin binding is marked with an arrow (→). The conserved sequence, Rx6DLPEF, has been shown to be essential for binding of several ADAMs (excluding ADAM10 and ADAM17) to the integrin $\alpha_9\beta_1$. MADAM contains a five amino acid insertion (NIHKM) with unknown significance within the integrin-binding region.

Specific Aims

As stated previously, little is known regarding how microsporidia invade host cells other than that polar tube extrusion must occur. Based on previous research, we hypothesize that adherence of microsporidia spores to the host cell surface is an event that may trigger polar tube extrusion and subsequent host cell infection. In an effort to better understand the mechanism of microsporidia spore adherence, we have turned our attention to determining what microsporidia proteins may be involved in this process. MADAM is a protein of interest given that it shares sequence homology with members of the ADAM family. ADAMs are involved in a variety of biological processes such as cell adhesion, proteolysis, cell fusion, and signaling. Ultimately, we would like to determine if MADAM is involved in microsporidia spore adherence and/or host cell infection and if so, what role does it play.

Our first objective is to determine the location of MADAM within the microsporidia spore by using immunoelectron microscopy. Localization of MADAM on the surface of the spore or in areas such as the anchoring-disk or polar tube would suggest that MADAM may be in a position to facilitate microsporidia adherence or polar tube extrusion. For our second objective we will use an already established *in vitro* system in order to assay if MADAM is involved in microsporidia adherence to the host cell and/or host cell infection. Our third objective is to identify potential substrates or binding partners for MADAM using a yeast two-hybrid approach. By completing these objectives, we should be able to develop a hypothesis regarding the potential role of MADAM within the microsporidia.

CHAPTER 2

MATERIALS AND METHODS

Microsporidia Spore Propagation and Purification

E. cuniculi and *E. intestinalis* were propagated in rabbit kidney cells (RK-13; ATCC CCL-37) or African green monkey kidney cells (Vero; ATCC CCI-81) as previously described (Hayman and Nash 1999). Briefly, subconfluent RK-13 or Vero monolayers grown in 75-cm² tissue culture flasks were incubated with either *E. cuniculi* or *E. intestinalis* spores for 10-12 days with growth medium replacement as needed. Cultures were maintained in 5% CO₂ at 37°C with growth medium consisting of Dulbecco's modified Eagle's medium (BioWhittaker; Walkersville, MD) supplemented with L-glutamine (2mM), penicillin (100U/ml), streptomycin (100µg/ml), amphotericin B (0.25µg/ml), and 2% fetal bovine serum (FBS). Spores were harvested by centrifugation at 3,500 RPM for 10 minutes and purified from the host cell debris by washing with 0.25% sodium dodecyl sulfate (SDS) followed by several washes in sterile water. Spores were counted and stored in sterile water at 4°C.

Cloning and Recombinant Expression of the *E. cuniculi* MADAM Protein

DNA encoding the region from the pro-domain to the transmembrane-domain or amino acids 21-527 of MADAM was amplified by PCR using genomic DNA from *E. cuniculi* infected RK-13 cells as the template and the following oligonucleotide primers: DIS-F1-E; 5'-GGAATTCTTCACTGACCCGGATGGTAAG-3' and DIS-R1-X; 5'-ACTCGAGTGTAGCTGCTGAATTGCTGTCTC-3'. The resulting PCR product was digested with EcoRI and XhoI then ligated into the linearized pET-21a vector (EMD Chemicals, Inc.; San Diego, CA) to generate the pET-21a+MADAM (Δ SS/ Δ TM) plasmid. *Escherichia coli* XLI-Blue (Stratagene; La Jolla, CA) was

used as the host strain for plasmid propagation. After verifying the DNA sequence, the pET-21a+MADAM (Δ SS/ Δ TM) plasmid was transformed into *E. coli* Rosetta-gami cells (EMD Chemicals, Inc.; San Diego, CA) for protein expression. Recombinant protein expression was induced at an OD₆₀₀ of approximately 0.6 by the addition of 1mM isopropyl- β -D-thiogalactopyranoside (IPTG) to the culture for 4 hours at 37°C with shaking. After induction, the bacteria were harvested, resuspended in binding buffer (1X phosphate buffer pH 7.4, 20mM Imidazole, and 8M urea), and lysed by sonication.

Protein lysate from induced and non-induced bacteria cultures was separated by sodium lauryl dodecyl sulfate-polyacrylamide gel electrophoresis (SDS-PAGE). Proteins were then stained with Coomassie Brilliant Blue R (Sigma-Aldrich; St. Louis, MO) or transferred to nitrocellulose membrane for Western analysis. Following the transfer, the membrane was blocked with 5% non-fat dry milk in 1X Tris buffered saline (TBS) pH 7.4 for 30 minutes. The membrane was then incubated for 1 hour in a 1:1,000 dilution of mouse monoclonal anti-polyhistidine antibody (Sigma-Aldrich; St. Louis, MO) prepared in TBS plus 0.05% Tween-20 (1X TBST) followed with a 1:2,000 dilution of rabbit anti-mouse alkaline phosphatase-conjugated antibody (Southern Biotech; Birmingham, AL) also prepared in 1X TBST. Colorimetric detection was performed using a combination of BCIP (5-bromo-4-chloro-3'-indolyphosphate p-toluidine salt) and NBT (nitro-blue tetrazolium chloride) (Pierce; Rockford, IL).

Purification of the Histidine-Tagged Recombinant MADAM Protein and Antibody Production

Purification of the rMADAM-His-Tag protein from *E. coli* was performed according to the manufacturer's protocol for the HiTrap HP Kit (GE Healthcare; Piscataway, NJ). Elution fractions containing rMADAM-His-Tag protein were combined, dialyzed overnight against

10mM Tris-HCl pH 7.5, and concentrated in a Centriplus centrifugal filter device (Millipore; Billerica, MA). Purified rMADAM-His-Tag protein was sent to Proteintech Group, Inc. (Chicago, IL) for polyclonal antibody production in two pre-screened rabbits. Following the 56-day antibody production protocol, total IgG antibodies were purified from the rabbit pre-bleed and final bleed sera according to the manufacturer's protocol for Immobilized Protein A/G Agarose (Pierce; Rockford, IL).

Western Analysis of *E. cuniculi* and *E. intestinalis* Spore Protein

Total protein was extracted from *E. cuniculi* and *E. intestinalis* spores by boiling for 15-30 minutes in the presence of lysis buffer (5% SDS, 60mM Tris-HCl pH 6.8, 10% glycerol) with fresh 2-mercaptoethanol (2-ME) added to a final concentration of 15% (v/v). After centrifugation at 13,000 RPM for 5 minutes to remove spore debris, the resulting protein lysate was separated by SDS-PAGE. For Western analysis, membranes were incubated in a 1:500 dilution of the anti-rMADAM-His-Tag antibody prepared in 1X TBST followed with a 1:2,000 dilution of goat anti-rabbit alkaline phosphatase-conjugated antibody (Southern Biotech; Birmingham, AL) also prepared in 1X TBST. Colorimetric detection was performed using a combination of BCIP and NBT.

Identification of the ~143kDa *E. cuniculi* Spore Protein

A sheet of nitrocellulose membrane was incubated for 1 hour with a 1:100 dilution of anti-rMADAM-His-Tag antibody prepared in 1X TBST. After blocking the membrane with 5% non-fat dry milk in 1X TBS, the membrane was incubated overnight in a solution of protein lysate extracted from *E. cuniculi* spores. Unbound *E. cuniculi* proteins were removed by washing in 1X TBST then the remaining *E. cuniculi* proteins were eluted in the presence of

lysis buffer (5% SDS, 60mM Tris-HCl pH 6.8, 10% glycerol) with fresh 2-ME added to a final concentration of 15% (v/v). The resulting protein sample, which represented *E. cuniculi* protein that specifically bound to anti-rMADAM-His-Tag antibody, was separated by SDS-PAGE. For Western analysis, membranes were incubated in a 1:500 dilution of the anti-rMADAM-His-Tag antibody prepared in TBST followed by a 1:2,000 dilution of goat anti-rabbit alkaline phosphatase-conjugated antibody (Southern Biotech; Birmingham, AL) also prepared in TBST. Colorimetric detection was performed using a combination of BCIP and NBT. The *E. cuniculi* protein band located at ~143kDa on the Coomassie stained gel was excised and sent to Midwest Bio Services, LLC (Overland Park, KS) for mass spectrometry analysis.

Immunolabeling and Transmission Electron Microscopy

RK-13 monolayers grown in T-75 cm² flasks were incubated with *E. cuniculi* or *E. intestinalis* spores until numerous infected foci could be observed. Infected RK-13 monolayers were fixed for 1 hour with 2% paraformaldehyde plus 0.05% glutaraldehyde in 0.2M Sorenson's buffer. Following several washes with 0.1M Sorenson's buffer, the monolayers were removed by scraping and enrobed in 3% SeaKem agar. The agar enrobed pellet was washed 3 times with 0.1M Sorenson's buffer at 4°C for 15 minutes. The pellet was sequentially dehydrated with 35% methanol, 50% methanol, 70% methanol at 4°C for 5 minutes and with 90% methanol at -20°C for 30 minutes. The following infiltration steps were performed for 1 hour at -20°C: 1:1 Lowicryl K4M resin/90% methanol, 2:1 Lowicryl K4M resin/90% methanol, and Lowicryl K4M resin only. The pellet was incubated in Lowicryl K4M resin overnight at -20°C. The pellet was then embedded in Lowicryl K4M resin

and photo-polymerization was carried out for 2 days at -20°C, 2 days at 4°C, and at room temperature for 2 days.

All solutions for immunolabeling were filter sterilized immediately prior to use. Gold thin sections were incubated in a blocking solution containing 1% albumin and 0.01M glycine prepared in phosphate buffered saline (PBS) for 5 minutes. The gold thin sections were then incubated with various dilutions of Protein A/G purified polyclonal rabbit antibody against the rMADAM-His-Tag protein prepared in blocking solution for 40 minutes at 37°C and washed with PBS three times for 5 minutes each. The gold thin sections were blocked again for 5 minutes then incubated for 30 minutes at 37°C with a 1:200 dilution of AuroProbe EM 15nm gold-labeled goat anti-rabbit IgG (H+L) (GE Healthcare; Piscataway, NJ). The gold thin sections were washed with PBS three times for 5 minutes followed by three fifteen minute washes with sterile water. The gold thin sections were counterstained with 5% uranyl acetate, washed with sterile water, and examined using a Tecnai 10 (FEI) transmission electron microscope.

Cloning, Recombinant Expression, and Purification of *E. cuniculi* MADAM Deletion Mutants

Primers were designed to PCR amplify the MADAM pro-domain (DIS-F1-E; 5'-GGAATTC T TCACTGACCCGGATGGTAAG-3' and DIS-R2-X; 5'-GTACTCGAGGACGTTTCCCTCCTCATC-3') and the MADAM metalloprotease-domain (DIS-F3-E; 5'-GGAATTCACAAGAGTCATCAAAGTG-3' and DIS-R3-X; 5'-GTACTCGAGTATCTCGCCAAATTTGGATTC-3'). Each PCR product was digested with EcoRI and XhoI then ligated into the pET-21a vector (EMD Chemicals, Inc.; San Diego, CA) to create the pET-21a+PRO and pET-21a+MET plasmids. *E. coli* XLI-Blue (Stratagene; La Jolla, CA) was used as the host strain for plasmid propagation. After verifying the DNA sequence, the pET-21a+PRO and pET-21a+MET plasmids were transformed into *E. coli*

Rosetta-gami cells (EMD Chemicals, Inc.; San Diego, CA). Protein expression was induced at an OD₆₀₀ of approximately 0.6 by the addition of 1mM IPTG to the culture for 4 hours at 37°C with shaking. After induction, the bacteria were harvested and resuspended in binding buffer (1X phosphate buffer pH 7.4, 20mM Imidazole, and 8M urea) then lysed by sonication. Purification of rMET-His-Tag protein and rPRO-His-Tag protein from the *E. coli* lysate was performed according to the manufacturer's protocol for the HiTrap HP Kit (GE Healthcare; Piscataway, NJ). Elution fractions were combined, dialyzed overnight against 10mM Tris-HCl pH 7.5, and concentrated in a Centriplus centrifugal filter device (Millipore; Billerica, MA).

Spore Adherence Assays

Spore adherence assays were performed as previously described (Hayman and others 2005). Briefly, Vero cells were seeded onto 18-mm glass coverslips at a density of 1×10^5 in 12-well plates with growth medium and allowed to grow to ~95% confluence. Recombinant protein was serially diluted ($1 \mu\text{g}/\text{ml}$ - $0.001 \mu\text{g}/\text{ml}$) in growth medium. The 12-well plate containing the Vero monolayers was placed on ice for 30 minutes. Following the 30-minute incubation, old medium was removed and 2ml of new medium containing various dilutions of recombinant protein plus ten million (10^7) *E. intestinalis* spores were added to each well. The 12-well plate was incubated on ice for 4 hours, then each coverslip was removed and washed thoroughly by repeatedly dunking the coverslips into phosphate buffered saline (PBS). The Vero monolayers and attached spores were fixed with a 50:50 solution of acetone:methanol for 10 minutes at room temperature. Indirect immunofluorescence assays (IFA) were then performed.

First, the monolayers were incubated in blocking buffer (5% FBS in PBS) for 30 minutes at room temperature. Rabbit antiserum, which recognizes *E. cuniculi* and *E. intestinalis* spores, was used as primary at a concentration of 1:1,000 in blocking buffer. Fluorescein isothiocyanate-conjugated (FITC) anti-rabbit IgG (Rockland Immunochemicals; Gilbertsville, PA) was used as secondary at a concentration of 1:2,000 in blocking buffer. The number of attached spores was counted in at least 10 different fields at a single magnification. Results are expressed as the mean +/- standard deviation or as the percentage of attached spores relative to the control. Statistical significance was determined using the Student's t-test.

Host Cell Infectivity Assays

Each spore adherence assay was set up in duplicate. While one set of coverslips was processed to measure spore adherence, the other set of coverslips was processed to measure infectivity. Following removal of the unbound spores, the coverslips for the infectivity assay were placed into a new 12-well plate with fresh medium. These Vero monolayers were incubated at 37°C in 5% CO₂ for ~36 hours in order to allow the attached spores to infect the host cells. Following this incubation, the coverslips were washed and fixed as in the spore adherence assay. The coverslips were then incubated in 0.01% Uvitex 2B (Polysciences, Inc.; Warrington, PA) for 10 minutes at room temperature. Uvitex 2B is a fluorescent dye that will bind to chitin in the microsporidia spore wall. After washing with PBS, the coverslips were inverted onto a microscope slide and sealed to prevent drying of the monolayer. Infected host cells were visualized at a magnification of 400X with a UV filter. The total number of host cells and number of infected host cells were counted in at least 10 different fields at a single magnification. Results are expressed as the percentage

of infected host cells per field of magnification. Statistical significance was determined using the Student's t-test. Each spore adherence and host cell infectivity assay was performed in triplicate.

Yeast Two-Hybrid Analysis

The yeast two-hybrid system is an *in vivo* method that can be used to identify novel protein interactions, analyze known protein-protein interactions, or to examine the interactions between specific protein domains (Maple and Moller 2007). The yeast two-hybrid system is based on the modular nature of eukaryotic transcription factors (Causier and Davies 2002). The Matchmaker™ Library Construction & Screening Kit (Clontech Laboratories, Inc.; Mountain View, CA) is a GAL4-based system. GAL4 is a yeast transcription factor involved in galactose metabolism. One domain known as the GAL4 DNA-binding domain (GAL4 DNA-BD) interacts with the appropriate DNA sequence within the promoter region, while the other domain is responsible for recruiting the transcriptional apparatus and is known as the activation domain (GAL4 AD). Although the GAL4 DNA-BD and GAL4 AD domains are structurally and functionally distinct, they can not activate transcription independently but instead must interact non-covalently in order to initiate transcription (Causier and Davies 2002).

In the Matchmaker™ yeast two-hybrid system, a plasmid encoding for a “bait” protein fused to the GAL4 DNA-BD is co-transformed into yeast with a plasmid that encodes for a “prey” protein fused to the GAL4 AD (Figure 7). If the “bait” and “prey” proteins interact, then the GAL4 DNA-BD and GAL4 AD are brought together and activity of the GAL4 transcription factor is restored. Activation of the GAL4 transcription factor ultimately leads to reporter gene expression, which is measured by nutritional selection (Figure 7).

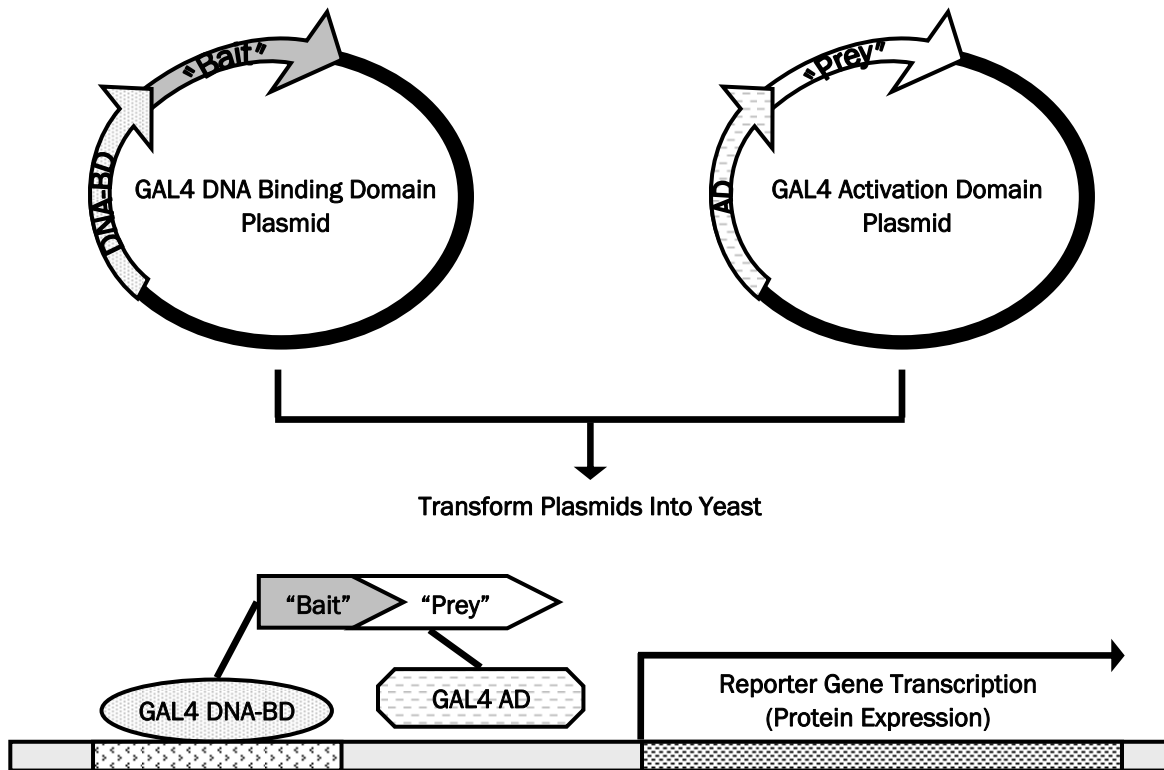


Figure 7 Diagram of yeast two-hybrid analysis. The GAL4 DNA-binding domain plasmid encodes for a “bait” protein fused to the GAL4 DNA-BD while the GAL4 activation domain plasmid encodes for a “prey” protein fused to the GAL4 AD. The “prey” can be a known protein or an unknown protein from a cDNA library. In either case, both plasmids are transformed into a suitable yeast strain. If the “bait” and “prey” proteins interact, then activity of the GAL4 transcription factor will be reconstituted and reporter gene expression will occur. Nutritional selection is often used as a measure of reporter gene expression.

Construction of GAL4 DNA-BD+MADAM Fusion Vectors

The first step in yeast two-hybrid analysis involves construction of a GAL4 DNA-BD plasmid that expresses the “bait” protein as a fusion with the GAL4 DNA-BD. The pGBKT7 vector (Figure 8) provided with the Matchmaker™ Library Construction & Screening Kit was used to generate a fusion protein between MADAM and the GAL4 DNA-BD. Our initial construct consisted of DNA corresponding to the MADAM pro-domain through the unknown region with deletion of the signal sequence and transmembrane domain (Figure 9). Deletion of the signal sequence and transmembrane domain ensures that neither will interfere with

localization of the GAL4 DNA-BD+MADAM fusion protein within the yeast. Subsequent constructs were generated by deleting the unknown region, disintegrin domain, and metalloprotease domain of MADAM (Figure 9). Primers were designed to introduce unique EcoRI and BamHI restriction sites at each end of the MADAM PCR product (Table 1). Each PCR product was digested, ligated into linearized pGBKT7 vector, and transformed into TOP10 *E. coli* cells (Invitrogen; Carlsbad, CA) for plasmid propagation.

A different cloning strategy was used to generate the pGBKT7+MADAM (Δ SS/ Δ MET/ Δ TM) plasmid (Figure 9). Primers (DIS-F1-SacI: 5'-GCGAGCTCGACACATGTGGAAACGGTATC-3' and DIS-R1-SacI: 5'-CGGAGCTCGACGTTTCCCTCCTCATCGTG-3') were designed to introduce a SacI restriction site at the beginning and end of the metalloprotease domain sequence within the MADAM gene. The pGBKT7+MADAM (Δ SS/ Δ TM) plasmid was used as template to generate the PCR product lacking the region corresponding to the metalloprotease domain. The PCR product was digested with SacI and ligated in order to re-circularize the DNA thus generating the pGBKT7+MADAM (Δ SS/ Δ MET/ Δ TM) plasmid. The plasmid was transformed into TOP10 *E. coli* cells. The sequence for pGBKT7+MADAM (Δ SS/ Δ MET/ Δ TM) plasmid was confirmed to ensure that the metalloprotease domain (amino acid 141-362) was deleted from the MADAM insert.

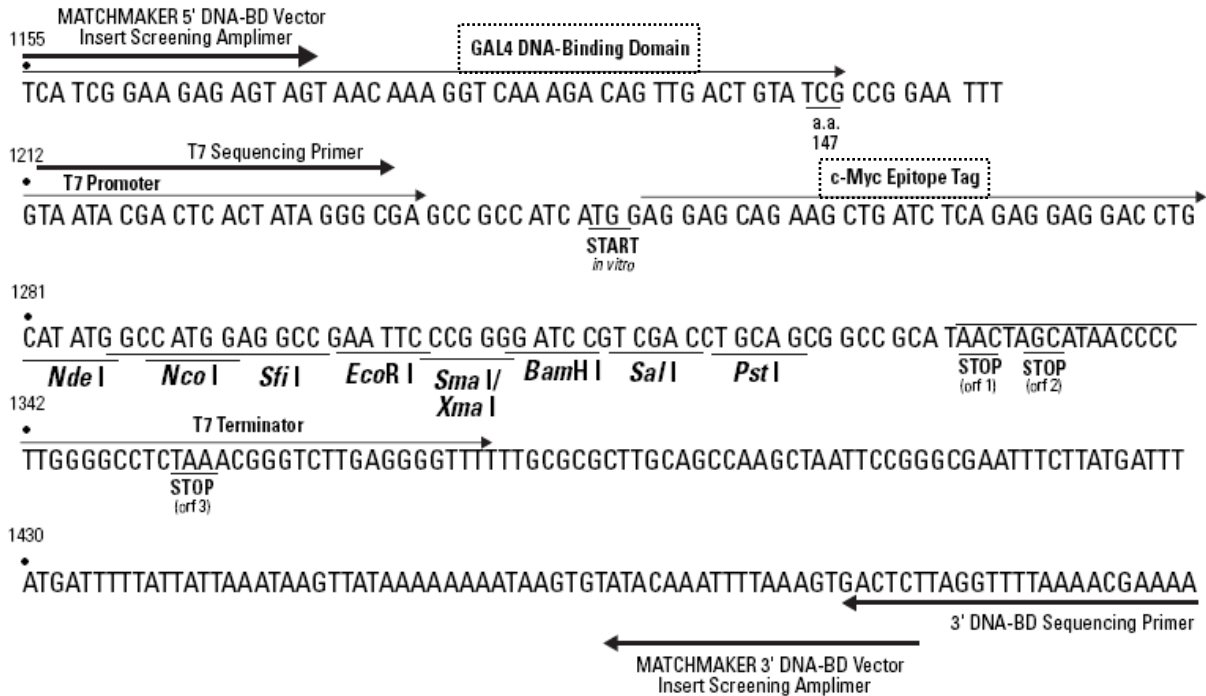
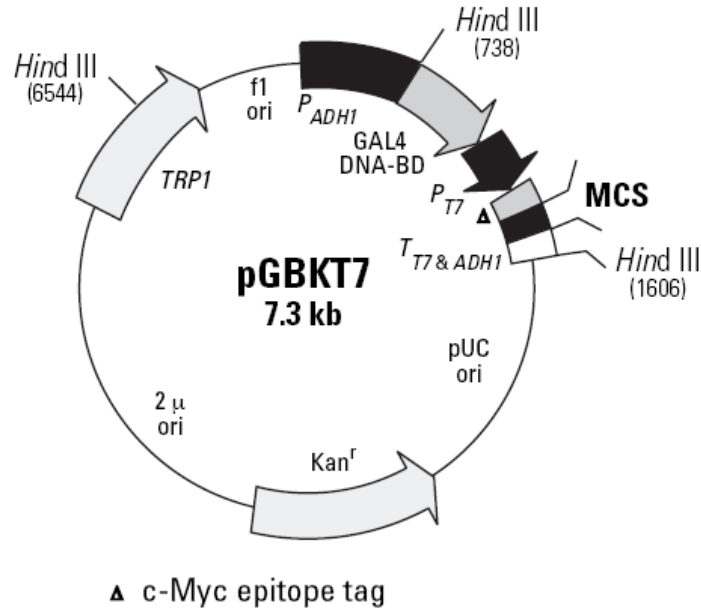


Figure 8 Diagram of the pGBKT7 vector. During our yeast two-hybrid analysis, the pGBKT7 vector was used to express MADAM protein fused to amino acids 1-147 of the GAL4 DNA binding domain (GAL4 DNA-BD). Each MADAM construct was inserted into the multiple cloning site (MCS) of the pGBKT7 vector. In yeast, expression from the constitutive ADH1 promoter (P_{ADH1}) results in a protein consisting of an N-terminal GAL4 DNA-BD followed by a c-Myc epitope tag (Δ) and the MADAM protein. The pGBKT7 vector carries an antibiotic resistance marker (Kan^r) for selection in *E. coli* and a nutritional marker (*TRP1*) for selection in yeast. (adapted from Maple and Moller 2007).

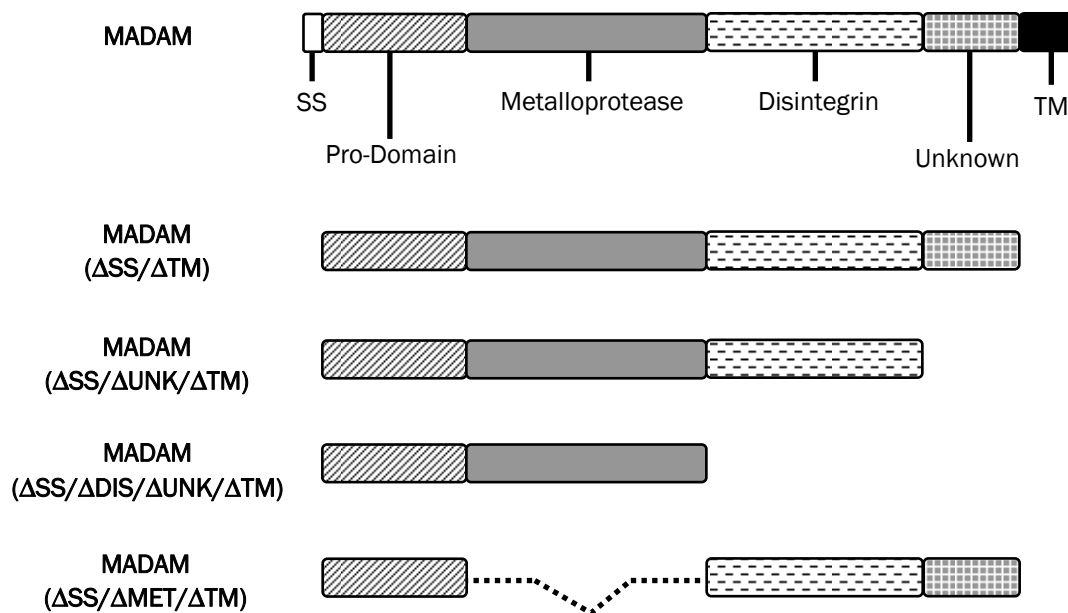


Figure 9 MADAM constructs used for yeast two-hybrid analysis. The domains of full-length MADAM protein are shown first followed by the deletion mutants constructed for insertion into the pGBKT7 vector. MADAM (Δ SS/ Δ TM) does not have the signal sequence (SS) or transmembrane domain (TM). MADAM (Δ SS/ Δ UNK/ Δ TM) does not have the SS, unknown region (UNK), or the TM. In addition, the MADAM (Δ SS/ Δ DIS/ Δ UNK/ Δ TM) construct does not possess the disintegrin domain (DIS). MADAM (Δ SS/ Δ MET/ Δ TM) was generated by deleting the metalloprotease domain (MET) and therefore consists of only the pro-domain, disintegrin domain, and unknown region. Primer sets used to generate the first three MADAM deletion constructs are listed in Table 1. The deletion mutants were generated in order to better characterize which domain or domains are involved in certain protein-protein interactions.

Table 1 Primers used to generate MADAM PCR products for insertion into the pGBKT7 vector.

Primer Set	Sequence (5' → 3')	Amplicon
DIS-F1-E	GGAATTCTTCACTGACCCGGATGGTAAG	MADAM
DIS-R1-BamH1	GACGGATTCTGTAGCTGCTGAATTGCTGTCTCTTTGG	Amino Acid 21-527
DIS-F1-E	GGAATTCTTCACTGACCCGGATGGTAAG	MADAM
DIS-R2-BamH1	GACGGATCCGGCACCATCGGAGACATATC	Amino Acid 21-453
DIS-F1-E	GGAATTCTTCACTGACCCGGATGGTAAG	MADAM
DIS-R3-BamH1	GACGGATCCTATCTCGCCAAATTTGGATTC	Amino Acid 21-362

Transformation of Yeast with the GAL4 DNA-BD+MADAM Fusion Vectors

Saccharomyces cerevisiae strain AH109 provided with the Matchmaker™ Library Construction & Screening Kit possesses 4 reporter genes (*ADE2*, *HIS3*, *MEL1*, and *lacZ*). The *ADE2* reporter alone allows for strong selection of yeast transformants grown on medium lacking adenine. A higher level of stringency is obtained when expression of the *HIS3* reporter is screened for in addition to the *ADE2* reporter by growing the yeast in medium lacking histidine and adenine. The *MEL1* reporter encodes for the secreted α -galactosidase enzyme, which provides the option of performing blue-white colony screening of the yeast transformants in the presence of the X- α -Gal substrate.

A small-scale yeast transformation procedure was performed to introduce each pGBKT7+MADAM plasmid independently into the AH109 yeast cells. Transformations were performed using a lithium acetate mediated method according to the Matchmaker™ Library Construction & Screening Kit (Clontech Laboratories, Inc.; Mountain View, CA). Yeast transformants were evaluated for growth on the following synthetic dropout (SD) minimal medium: SD/-Trp, SD/-Trp/-His, and SD/-Trp/-Ade.

Generation of the cDNA Library from *E. intestinalis*-Infected Vero Host Cells

The Matchmaker™ Library Construction & Screening Kit was used to generate a cDNA library from *E. intestinalis*-infected Vero cells. A Vero monolayer grown in a T-75 cm² flask was incubated with *E. intestinalis* spores until numerous infected foci could be observed. Total RNA was isolated from the *E. intestinalis*-infected Vero cells using an RNeasy Mini Kit (QIAGEN; Valencia, CA). RNA quality was assessed with the Agilent

Bioanalyzer by the Molecular Biology Core Facility (East Tennessee State University; Johnson City, TN).

The Matchmaker™ system employs the SMART (Switching Mechanism at 5' end of RNA Transcript) technology in order to copy mRNA transcripts into double stranded cDNA (ds cDNA). First-strand cDNA synthesis was accomplished using Moloney Murine Leukemia Virus Reverse Transcriptase (MMLV RT) and total RNA isolated from the *E. intestinalis*-infected Vero cells. The CDS III/6 random primer (5'-ATTCTAGAGGCCGAGGCGGCCGACATG-NNNNNN-3' where N=A, G, C, or T) was used to prime the RNA for cDNA synthesis (Figure 2.4). In contrast to the oligo(dT) primer (CDS III), which only hybridizes to the poly A+ tail at the 3'-end of the RNA, the CDS III/6 primer will hybridize to many different sequences on the RNA template.

During first-strand synthesis, MMLV RT encounters the 5'-end of the RNA template and with its terminal transferase activity will add a deoxycytidine (dC) stretch to the 3'-end of the newly synthesized single stranded cDNA (Figure 10). An extended template is generated by the addition of SMART III™ Oligonucleotide (5'-AAGCAGTGGTATCAACGCAGAGTGGCCATTATGGCCGGG-3'), which base-pairs with the dC stretch (Figure 2.4). MMLV RT switches templates and continues to replicate to the end of the SMART III™ Oligonucleotide. Only ss cDNA with the SMART III™ oligonucleotide sequence at the 5'-end can serve as a template to be exponentially amplified by long-distance PCR (LD-PCR) to produce the ds cDNA. During LD-PCR of the *E. intestinalis*+Vero cDNA, the 5' PCR Primer (5'-TTCCACCCAAGCAGTGGTATCAACGCAGAGTGG-3') and 3' PCR Primer (5'-GTATCGATGCCACCCTCTAGAGGCCGAGGCGGCCGACA-3') were used to amplify the cDNA and to complete the SMART III™ and CDS III anchors. Following amplification, the *E. intestinalis*+Vero ds cDNA library was

purified using a CHROMA SPIN™ TE-400 Column (Clontech Laboratories, Inc.; Mountain View, CA).

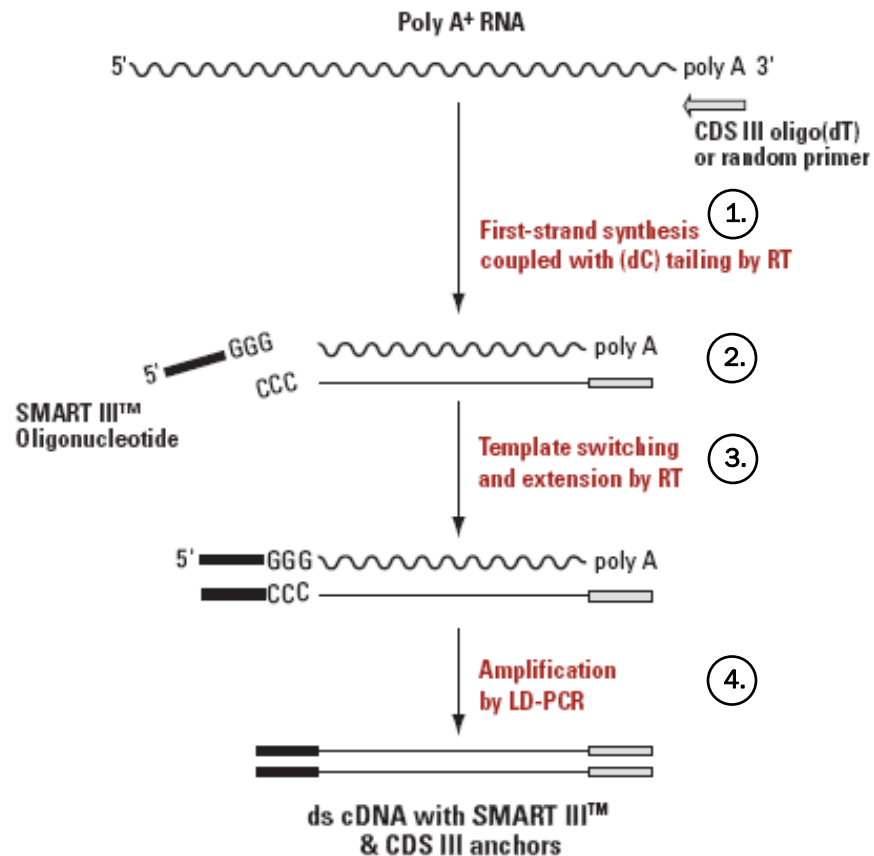
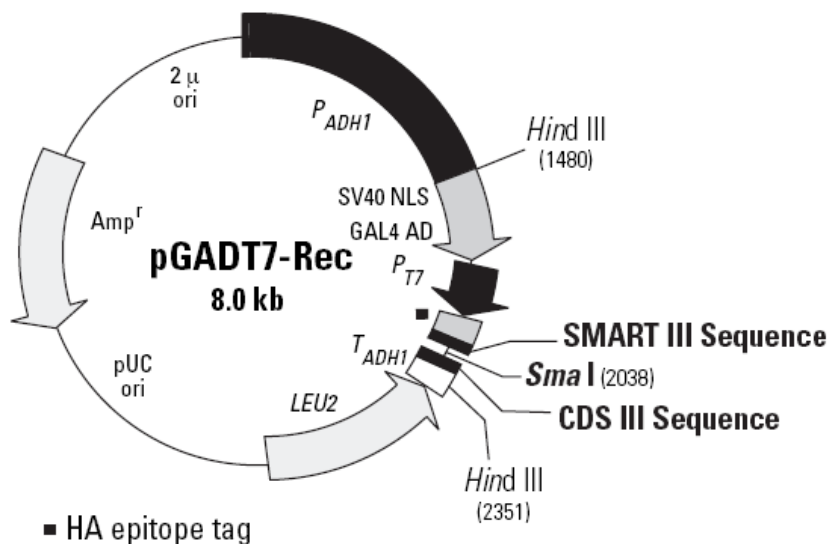


Figure 10 Synthesis of ds cDNA using the SMART™ technology. (1) During first strand synthesis, reverse transcriptase (RT) is used to transcribe the mRNA into cDNA. Either a modified oligo(dT) (CDS III primer) or random primer (CDS III/6 primer) can be used to prime the RNA for cDNA synthesis. When RT encounters the 5'-end of the RNA, the terminal transferase activity of the enzyme will add a deoxycytidine (dC) stretch to the 3'-end of the single-stranded cDNA (ss cDNA). (2) The SMART III™ oligonucleotide contains an oligo(G) sequence at its 3'-end that will base-pair with the dC stretch on the ss cDNA. (3) RT will switch templates and continue replicating to the end of the SMART III™ oligonucleotide. (4) Only ss cDNA with the SMART III™ oligonucleotide sequence at the 5'-end can serve as a template during long-distance PCR (LD-PCR). LD-PCR of the ss cDNA results in the generation of double-stranded cDNA (ds cDNA) with complete SMART III™ and CDS III anchors. (adapted from Zhu and others 2001).

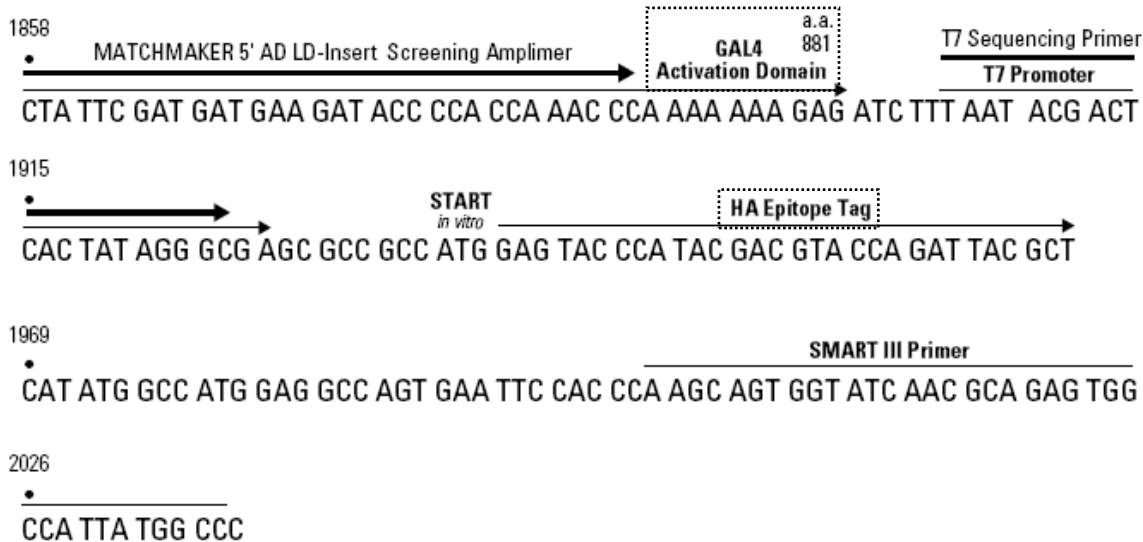
Construction of the GAL4 AD+cDNA Library Fusion Vectors

The pGADT7-Rec vector (Figure 11) provided with the Matchmaker™Library Construction & Screening Kit was used to generate fusion proteins between the *E. intestinalis*+Vero ds cDNA and the GAL4 AD. When the SMART ds cDNA and SmaI linearized pGADT7-Rec vector are co-transformed into the yeast, the ds cDNA will recombine with the pGADT7-Rec vector to yield the complete GAL4 AD+cDNA library plasmid (Figure 12). The GAL4 AD+cDNA library plasmid will express the cDNA insert as a fusion with the GAL4 AD. Recombination is possible because the SMART III and CDS III sequences that were incorporated into the cDNA are also engineered into the pGADT7-Rec vector. Yeast repair enzymes will restore the SmaI linearized pGADT7-Rec vector to its circular form by recombining the SMART III and CDS III homologous ends present in the cDNA and vector. Successful constitution of the pGADT7-Rec+cDNA plasmid can be determined by growth of the yeast on SD/-Leu medium.

The yeast transformation procedure was performed to introduce the SmaI linearized pGADT7-Rec vector and *E. intestinalis*+Vero ds cDNA into AH109 yeast cells that already contained the pGBKT7+MADAM (Δ SS/ Δ TM) plasmid. Transformations were performed using a lithium acetate mediated method according to the Matchmaker™Library Construction & Screening Kit (Clontech Laboratories, Inc.; Mountain View, CA). Yeast transformants were evaluated for growth on the following synthetic dropout (SD) minimal medium: SD/-Leu/-Trp (double dropout or DDO) and SD/-Leu/-Trp/-His (triple dropout or TDO).



SMART III™ terminus



CDS III terminus

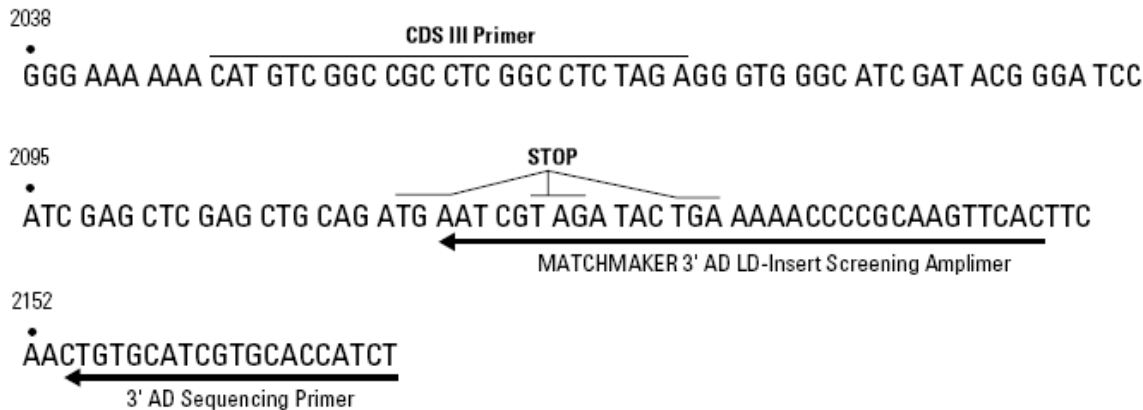


Figure 11 Diagram of the pGADT7-Rec vector (continued on page 43).

Figure 11 Diagram of the pGADT7-Rec vector. During our yeast two-hybrid analysis, the pGADT7-Rec vector was used to express the *E. intestinalis*+Vero cDNA library as a fusion with the GAL4 activation domain (GAL4 AD). The GAL4 AD+cDNA fusions expressed from the pGADT7-Rec vector will possess a hemagglutinin (HA) epitope tag (■). The pGADT7-Rec vector carries an antibiotic resistance marker (*Amp^r*) for selection in *E. coli* and a nutritional marker (*LEU2*) for selection in yeast. (adapted from Maple and Moller 2007).

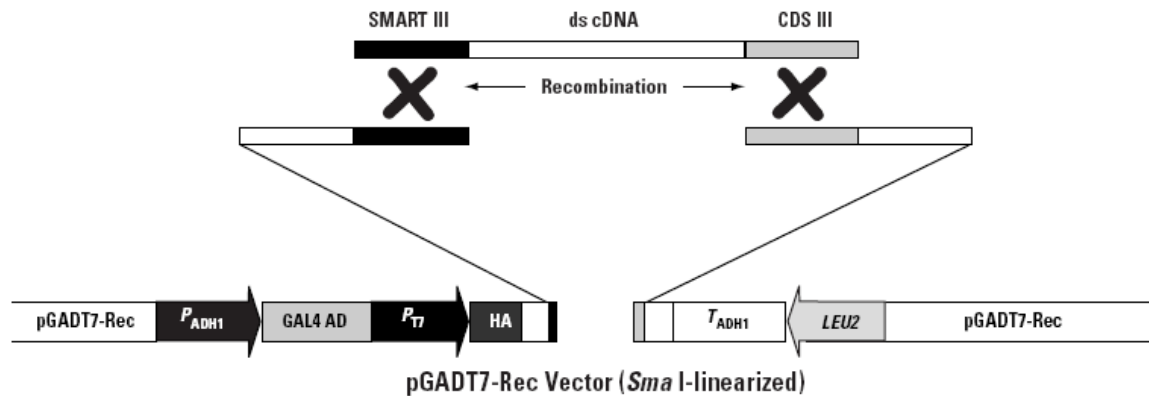


Figure 12 Homologous recombination of ds cDNA and the pGADT7-Rec vector. To introduce the ds cDNA into the pGADT7-Rec vector, first SMART III and CDS III sequences must be generated on the 5'- and 3'-terminal of the ds cDNA. When co-transformed into yeast, the ds cDNA will recombine with the pGADT7-Rec linearized vector thereby restoring the circular topology of the vector. (adapted from Clontech 2007).

Analysis of Positive Yeast Two-Hybrid Interactions

Growth of the yeast transformants on TDO medium indicated a potential positive interaction involving the GAL4 DNA-BD+MADAM (Δ SS/ Δ TM) protein and a GAL4 AD+cDNA fusion protein. Positive yeast transformants were transferred to fresh TDO medium for short-term storage. Each cDNA insert was amplified directly from the yeast colony using a technique known as PCR Colony Screening. This procedure uses the Matchmaker™ GAL4 AD LD-Insert Screening Amplimer Set (Forward PCR Primer: 5'-TTCCACCCAAGCAGTGGTATCAA CGCAGAGTGG-3 and Reverse PCR Primer: 5'-GTATCGATGCCACCCTCTAGAGGCCGAGGCGGC

CGAC A-3') and Advantage® 2 PCR Polymerase Mix (Clontech Laboratories, Inc.; Mountain View, CA) to PCR amplify the insert from the pGADT7-Rec+cDNA vector within the yeast colony. PCR amplification of the cDNA insert directly from the yeast colony provides an efficient preliminary screening method prior to proceeding with plasmid isolation from each positive yeast clone, which is costly and time consuming.

Each PCR product was analyzed by electrophoresis on 0.7% agarose impregnated with ethidium bromide (0.5µg/ml). PCR products that appeared to consist of a single DNA band were purified using the QIAquick PCR Purification Kit (QIAGEN; Valencia, CA) and sent to the Molecular Biology Core Facility (East Tennessee State University; Johnson City, TN) for DNA sequencing. Each chromatogram was manually inspected for evidence of poor DNA sequencing results. If the DNA sequence was usable, then the in-frame DNA sequence corresponding to the cDNA insert was translated to the appropriate protein sequence using ExPASy's Translate Tool (Gasteiger and others 2003). The translated protein sequence was analyzed using the Basic Local Alignment Tool (BLAST) to determine protein identification (Altschul and others 1990).

A yeast cell can stably maintain more than one plasmid. Therefore, yeast two-hybrid screening can lead to a yeast cell transformed with multiple pGADT7-Rec+cDNA plasmids. PCR Colony Screening revealed that 56% of the positive yeast transformants from our yeast two-hybrid screen actually contained multiple pGADT7-Rec+cDNA plasmids. Often only one of the plasmids is responsible for the positive interaction while the others are contaminating plasmids (Vidalain and others 2004). The presence of more than one pGADT7-Rec+cDNA vector within a single yeast colony will impair identification of the cDNA insert because multiple PCR bands will result in an unreadable DNA sequence. In an attempt to select for the correct plasmid, all of the positive yeast transformants were grown under positive

selection pressure by replica plating on TDO medium every 3 days for 15 days as previously described (Vidalain and others 2004). After replica plating, the yeast colonies were PCR screened again to determine if potential contaminating pGADT7-Rec+cDNA plasmids were lost.

pGADT7-Rec+cDNA insert and pGBKT7+MADAM (Δ SS/ Δ TM) plasmids were isolated from several yeast colonies using the Yeastmaker™ Yeast Plasmid Isolation Kit (Clontech Laboratories, Inc.; Mountain View, CA). pGADT7-Rec and pGBKT7 vectors contain different antibiotic selection markers. pGADT7-Rec+cDNA insert and pGBKT7+MADAM (Δ SS/ Δ TM) plasmids isolated from the yeast colonies were transformed and segregated in *E. coli*. Individual pGADT7-Rec+cDNA insert plasmids were isolated from the *E. coli* and re-transformed into AH109 yeast. Transformation of individual pGADT7-Rec+cDNA insert plasmids into the yeast allowed for the evaluation of reporter gene expression in the absence of the pGBKT7+MADAM (Δ SS/ Δ TM) plasmid. In addition, positive interactions were confirmed by co-transformation of yeast with certain pGADT7-Rec+cDNA insert plasmids and various pGBKT7+MADAM plasmids.

Construction of the GAL4 AD+Polar Tube Protein 1, 2, and 3 Fusion Vectors

The Matchmaker™ Library Construction & Screening Kit provides the components necessary to introduce ds cDNA into the SmaI linearized pGADT7-Rec vector. However, we were interested in introducing genes specific for the polar tube proteins into the pGADT7-Rec vector for yeast two-hybrid analysis. To accomplish this, we used primers to introduce the SMART III sequence to the 5'-terminal and the CDS III sequence to the 3'-terminal of each PCR product. By introducing these sequences, the genes could be directly inserted into the pGADT7-Rec vector by recombination-mediated cloning in the yeast cells. The first

round of PCR used primers that were primarily specific for the gene of interest but also contained 25 bases corresponding to the SMART III sequence for the forward primer and 21 bases corresponding to the CDS III sequence for the reverse primer (Table 2). A second round of PCR was used to finish the SMART III and CDS III anchor sequences using the Forward PCR Primer: 5'-TTCCACCCAAGCAGTGGTATCAACGCAGAGTGG-3' and Reverse PCR Primer: 5'-GTATCGATGCCACCCTCTAGAGGCCGAGGCCGCGACA-3'. A small-scale yeast transformation procedure was performed to introduce the SmaI linearized pGADT7-Rec vector and each individual *E. cuniculi* or *E. intestinalis* polar tube protein PCR product into AH109 yeast cells that already contained the pGBKT7+MADAM (Δ SS/ Δ TM) vector. Yeast transformations were performed using the lithium acetate mediated method according to the Matchmaker™ Library Construction & Screening Kit (Clontech Laboratories, Inc.; Mountain View, CA). Yeast transformants were evaluated for growth on DDO, TDO, and QDO medium.

Table 2 Primer used to generate *E. cuniculi* and *E. intestinalis* polar tube protein PCR products for insertion into the pGADT7-Rec vector.

Primer Set	Sequence (5' → 3')	Amplicon
EcPTP1-F1	<u>CAAGCGAGAGTGGCCATTATGGCCCATGAAAGGTATTTCTAAG</u>	<i>E. cuniculi</i> PTP1 (ECU06_0250)
EcPTP1-R1	<u>GAGGCCGAGGCGGCCGACATGGCAGCATTGGACAGCAGTG</u>	Amino Acid 1-395
EcPTP2-F1	<u>CAAGCGAGAGTGGCCATTATGGCCCATGTTGTTACTTCTCGCC</u>	<i>E. cuniculi</i> PTP2 (ECU06_0240)
EcPTP2-R1	<u>GAGGCCGAGGCGGCCGACATGCTCTAGACCCTCGCCGTC</u>	Amino Acid 1-277
EcPTP3-F2	<u>CAAGCGAGAGTGGCCATTATGGCCCGTGGGGGATCCATTCCC</u>	<i>E. cuniculi</i> PTP3 (ECU11_1440)
EcPTP3-R2	<u>GAGGCCGAGGCGGCCGACATGCCGGCCTTTGCCGCCTC</u>	Amino Acid 141-574
EiPTP1-F1	<u>CAAGCGAGAGTGGCCATTATGGCCCATGAAAGGTATTTCTAAGG</u>	<i>E. intestinalis</i> PTP1 (AJ880382)
EiPTP1-R1	<u>GAGGCCGAGGCGGCCGACATGGCATGGTGGTGGGCAGCAAGC</u>	Amino Acid 1-371
EiPTP2-F1	<u>CAAGCGAGAGTGGCCATTATGGCCCATGTTGTTACTTCTCAAGC</u>	<i>E. intestinalis</i> PTP2 (AX007052)
EiPTP2-R1	<u>GAGGCCGAGGCGGCCGACATGCTCTAGACCCTCGCCGTC</u>	Amino Acid 1-275

* Underlined bases represent either the SMART III™ terminal sequence (forward primer) or the CDS III terminal sequence (reverse primer). Introducing the SMART III™ and CDS III anchors allows for recombination of the PCR product with the pGADT7-Rec vector *in vivo*.

In vitro Transcription, Translation, and Co-Immunoprecipitation

Protein-protein interactions identified during our yeast two-hybrid screening were confirmed using *in vitro* transcription/translation and co-immunoprecipitation (Figure 13). The pGBKT7 and pGADT7-Rec vectors can be used directly for *in vitro* transcription, translation, and co-immunoprecipitation procedures because they possess a T7 RNA polymerase promoter and either a c-Myc (pGBKT7) or HA (pGADT7-Rec) epitope tag. Because the T7 promoter is located downstream of the GAL4 coding sequence, the proteins expressed during the *in vitro* procedures will not contain the GAL4 DNA-BD or GAL4 AD. *In vitro* transcription and translation were accomplished using the PROTEINSCRIPT® II Kit (Ambion, Inc.; Austin, TX). Briefly, transcription with the T7 bacteriophage RNA polymerase was followed by translation in an optimized rabbit reticulocyte lysate. *In vitro* translated proteins were labeled with L-[³⁵S]-methionine (GE Healthcare; Piscataway, NJ).

In vitro co-immunoprecipitation was performed using the Matchmaker™ Co-IP Kit (Clontech Laboratories, Inc.; Mountain View, CA). Briefly, the *in vitro* translated ³⁵S-methionine labeled “bait” and “prey” proteins were combined and incubated at room temperature for 1 hour. Depending on the experiment, either the c-Myc Monoclonal Antibody or HA-Tag Polyclonal Antibody was added and incubated with the reaction for 1 hour. Immunoprecipitation was accomplished by the addition of Protein A Beads followed by a 1 hour incubation at room temperature. Unbound proteins were removed by extensive washing of the Protein A Beads. Any remaining protein-protein-antibody complexes were removed from the Protein A Beads by heating in the presence of SDS-PAGE Loading Buffer. The proteins were analyzed by SDS-PAGE followed by autoradiography.

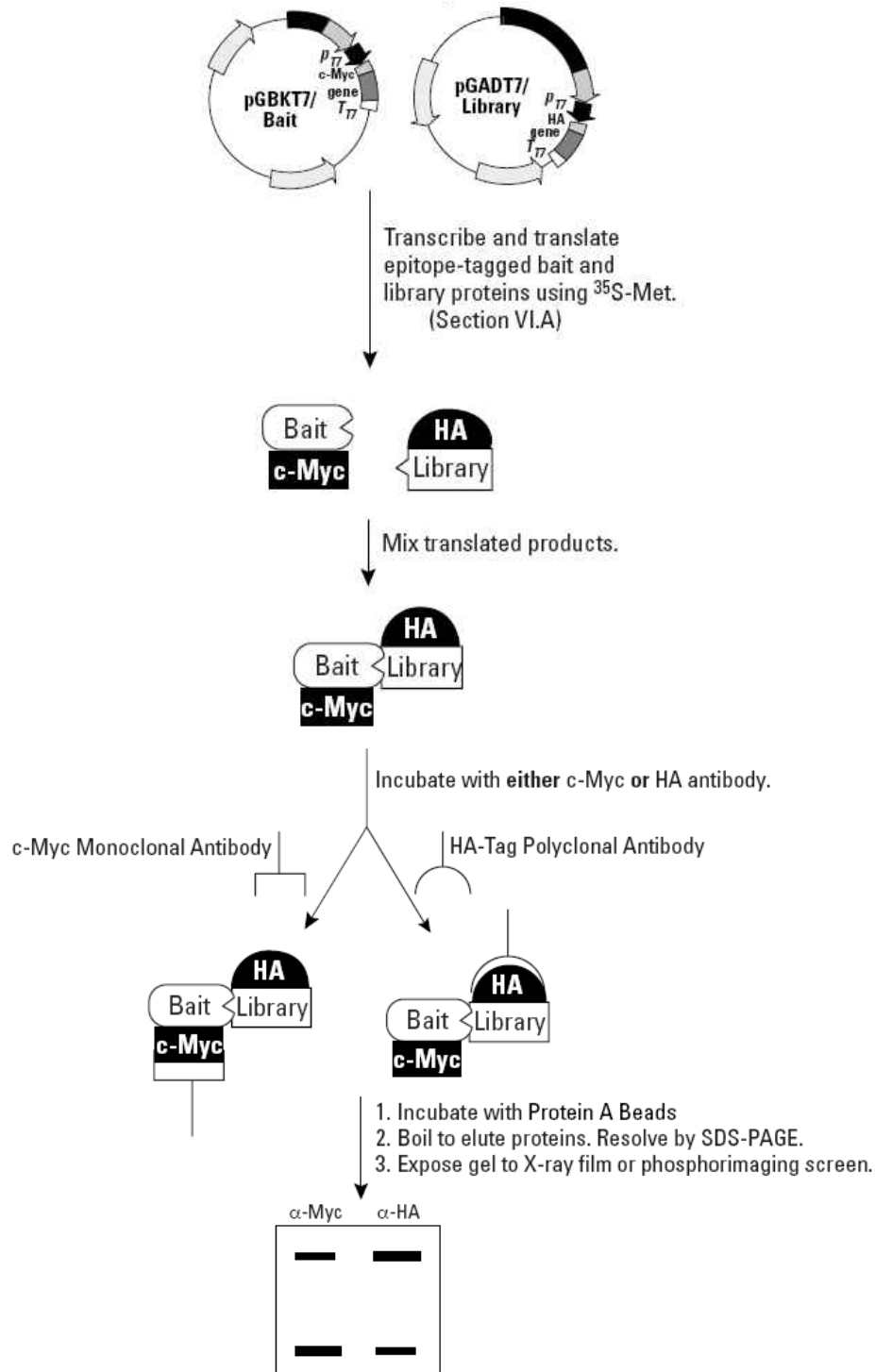


Figure 13 Overview of *in vitro* transcription, translation, and co-immunoprecipitation. Protein interactions identified during our yeast two-hybrid screen were confirmed using *in vitro* methods. ³⁵S-labeled proteins were generated from the pGBKT7+MADAM and pGADT7-Rec+cDNA plasmids using *in vitro* transcription and translation procedures. Protein interactions were confirmed using co-immunoprecipitation procedures according to the Matchmaker™ Co-IP Kit. (adapted from Clontech 2006).

CHAPTER 3

RESULTS

Recombinant Expression of MADAM Protein for Polyclonal Antibody Production

To begin characterization of the MADAM protein, a histidine-tagged recombinant MADAM (rMADAM-His-Tag) protein was expressed in *E. coli*. Protein lysate collected from non-induced and induced *E. coli* cultures that contain the pET-21a+MADAM (Δ SS/ Δ TM) plasmid were analyzed by SDS-PAGE and Western blot (Figure 14). Upon induction with IPTG, the *E. coli* produced a protein with an apparent molecular weight of ~61kDa which is comparable to the predicted size of ~59kDa for the rMADAM-His-Tag protein and was specifically recognized by the anti-His-Tag antibody.

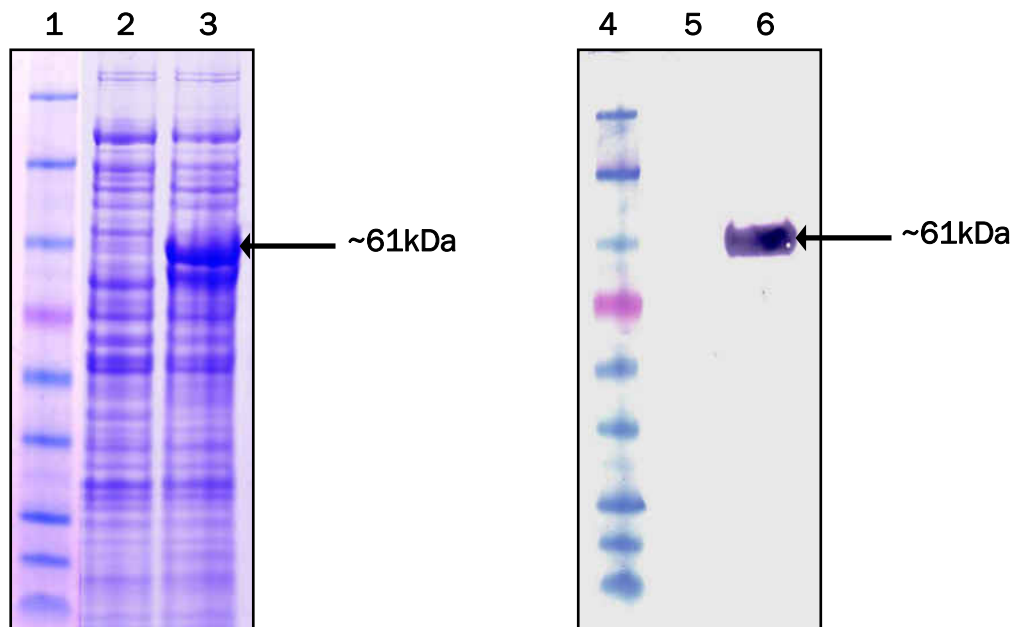


Figure 14 Expression of rMADAM-His-Tag protein. Protein lysate from the *E. coli* cultures were separated by SDS-PAGE and either stained with Coomassie Brilliant Blue R (Lane 1-3) or processed for Western analysis (Lane 4-6) using an anti-His-Tag antibody. Upon induction with IPTG, a protein of ~61kDa was observed (Lane 3) and this protein was specifically recognized by the anti-His-Tag antibody (Lane 6). The rMADAM-His-Tag protein was not observed in the non-induced *E. coli* protein lysate (Lane 2 and Lane 5). The molecular weight markers are in Lane 1 and Lane 4.

Western Analysis of MADAM Protein from *E. cuniculi* and *E. intestinalis*

Following confirmation of rMADAM-His-Tag protein expression, several milligrams of the rMADAM-His-Tag protein was purified by nickel affinity chromatography and used as antigen for polyclonal antibody production in rabbits. Total IgG antibodies were purified from the rabbit serum and used for Western analysis of *E. cuniculi* and *E. intestinalis* spore protein in order to determine specificity. Full-length MADAM protein from *E. cuniculi* is predicted to be ~61kDa. After removal of the signal sequence, the MADAM protein should be ~59kDa. Antibodies generated against the rMADAM-His-Tag protein did recognize a protein of ~60kDa from both *E. cuniculi* and *E. intestinalis* (Figure 15). However, these antibodies also recognized a protein of ~143kDa from *E. cuniculi* and *E. intestinalis* spores (Figure 15).

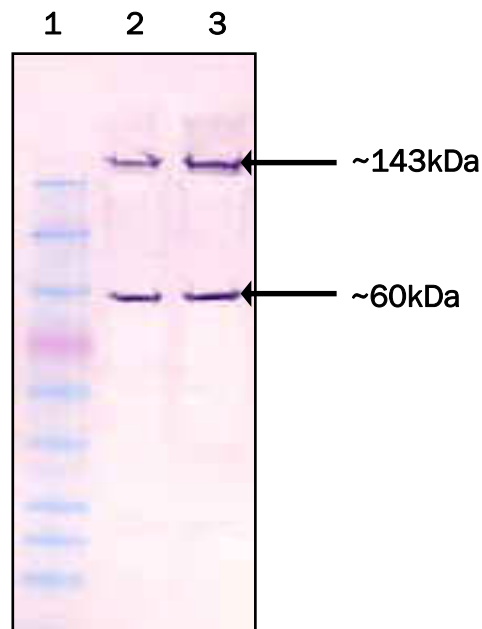


Figure 15 Western analysis of MADAM protein. Protein lysates from *E. cuniculi* (Lane 2) and *E. intestinalis* (Lane 3) spores were separated by SDS-PAGE then processed for Western analysis. Antibodies generated against the rMADAM-His-Tag protein recognized proteins of ~61kDa and ~143kDa from both *E. cuniculi* and *E. intestinalis*. MADAM protein from *E. cuniculi* is predicted to be ~61kDa or ~59kDa after removal of the signal sequence. The molecular weight markers are in Lane 1.

Identification of the ~143kDa Protein Recognized by the Anti-rMADAM-HisTag Antibodies

Mass-spectrometry based proteomics is one of the more common experimental approaches used to identify individual proteins within a complex protein mixture (Aebersold and Mann 2003). Purification of individual proteins within a sample is accomplished by techniques such as two-dimensional polyacrylamide gel electrophoresis (2D-PAGE) or immunoprecipitation if a specific antibody is available. Following the purification step, individual proteins are separated by SDS-PAGE and proteins spots or bands are excised from the gel. Digestion of the protein into peptides is followed by mass-spectrometry analysis. The protein is identified by matching the peptide sequences against a protein sequence database.

Unfortunately, attempts to separate the *E. cuniculi* spore proteins by 2D-PAGE in order to identify the ~143kDa *E. cuniculi* protein recognized by the anti-rMADAM-HisTag antibody were unsuccessful (data not shown). Also, we were unable to purify the ~143kDa *E. cuniculi* protein using a classical immunoprecipitation approach (data not shown). However, we were able to purify the ~143kDa *E. cuniculi* protein by incubating total protein lysate from *E. cuniculi* spores with a piece of nitrocellulose membrane that was pre-incubated with the anti-rMADAM-HisTag antibody. *E. cuniculi* proteins that bound to the antibody on the membrane were separated by SDS-PAGE and either stained with Coomassie Brilliant Blue R or processed for Western analysis. The *E. cuniculi* protein at ~143kDa was excised from the Coomassie stained gel and was sent for mass-spectrometry and protein sequence database analysis (Figure 16). The protein was identified as *E. cuniculi* polar tube protein 3 (PTP3). PTP3 has a predicted molecular weight of ~136kDa and has been shown to run at ~150kDa by SDS-PAGE (Peuvel and others 2002).

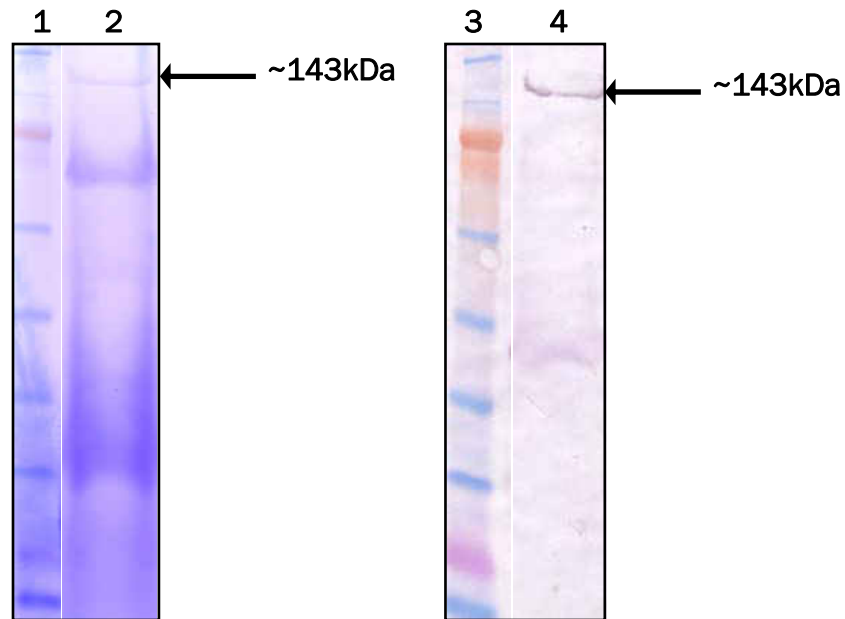


Figure 16 Purification and Identification of the ~143kDa *E. cuniculi* protein. A piece of nitrocellulose membrane pre-incubated with anti-rMADAM-His-Tag antibody was incubated with protein lysate from *E. cuniculi*. Proteins that did not interact with the antibody were washed away while the bound *E. cuniculi* proteins were eluted. The proteins were then separated by SDS-PAGE and either stained with Coomassie Brilliant Blue R (Lane 2) or processed for Western analysis (Lane 4) using the anti-rMADAM-His-Tag antibody. As observed in Lane 2 and 4, the ~143kDa protein was isolated. The protein band at ~143kDa in Lane 2 was excised and sent to Midwest Bio Services, LLC (Overland Park, KS) for mass spectrometry analysis. The protein was identified as *E. cuniculi* polar tube protein 3 (PTP3). The molecular weight markers are in Lane 1 and Lane 3.

Further examination of the pre-screened rabbit serum demonstrated that the rabbit already had antibodies against a protein of the same molecular weight as the ~143kDa protein or presumably PTP3 (Figure 17). Antibodies from the rabbit pre-immune serum did not react with the rMADAM-His-Tag protein, which indicates that this rabbit did not have antibodies against MADAM prior to immunization (Figure 17). The initial Western analysis of the rabbit pre-immune serum did not uncover this high molecular weight protein. Isolation of protein from microsporidia spores is not trivial and results can vary depending on factors such as spore stock, composition of the lysis buffer, and boiling conditions.

Microsporidia, particularly *E. cuniculi*, naturally infect rabbits and finding a naïve rabbit for antibody production will continue to be a challenge. In fact, western analysis of several other pre-immune sera from the same company and another company demonstrated that the rabbits already possess antibodies to various proteins from both *E. cuniculi* and *E. intestinalis* (data not shown). Future attempts to generate anti-rMADAM-HisTag antibody will be accomplished in rodents.

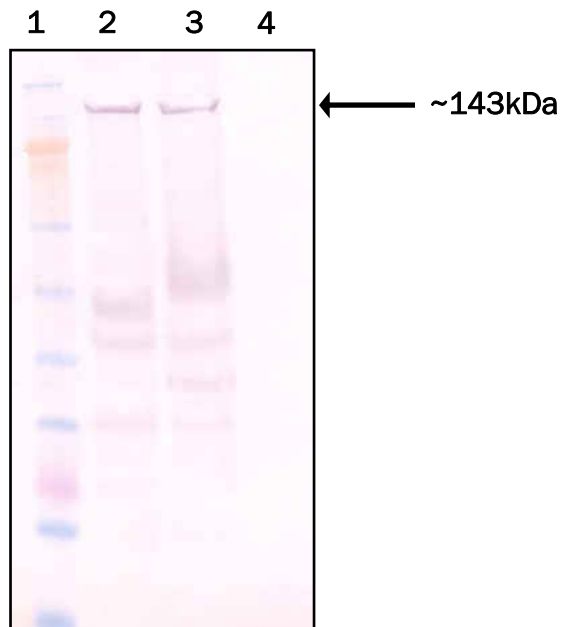


Figure 17 Western analysis of *E. cuniculi* and *E. intestinalis* protein using the rabbit pre-immune serum. Protein lysates from *E. cuniculi* (Lane 2) and *E. intestinalis* (Lane 3) spores were separated by SDS-PAGE then processed for Western analysis. Antibodies from the rabbit pre-immune serum recognize protein at ~143kDa from *E. cuniculi* and *E. intestinalis*. However, these antibodies do not recognize the rMADAM-HisTag protein (Lane 4). The molecular weight markers are in Lane 1.

Localization of the MADAM Protein within *E. cuniculi* and *E. intestinalis*

Immunoelectron microscopy was performed on *E. cuniculi* and *E. intestinalis* infected RK-13 cells using the anti-rMADAM-His-Tag antibodies to determine the location of the MADAM protein within the spore. As a control, immunolabeling was first performed using antibodies purified from the pre-immune serum. Although antibodies from the pre-immune serum reacted with *E. cuniculi* and *E. intestinalis* proteins by Western analysis, no specific labeling of the microsporidia was observed by TEM (Figure 18).

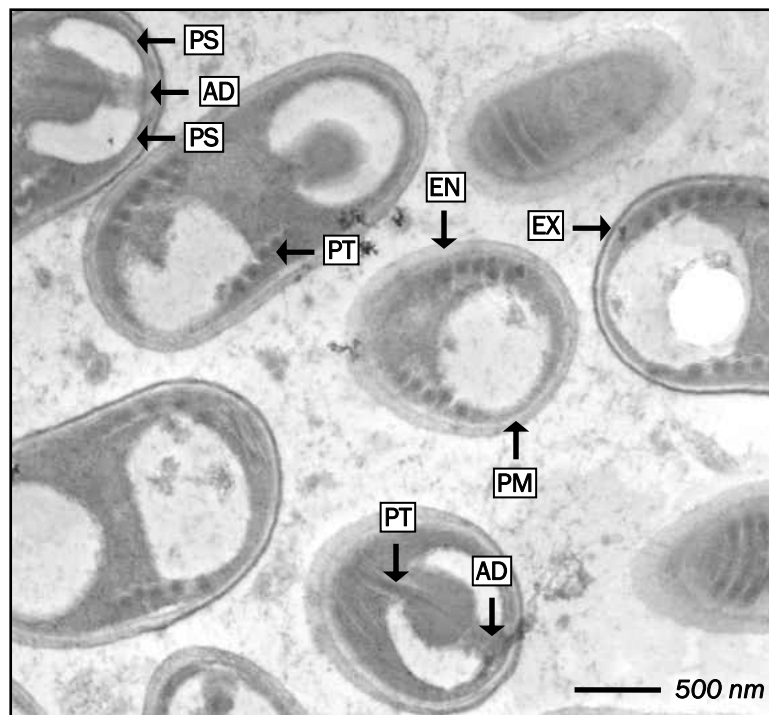


Figure 18 Immunolabeling of *E. intestinalis* infected RK-13 cells using antibodies from the pre-immune serum. Sections of *E. intestinalis* infected RK-13 cells were immunolabeled with antibodies from the rabbit pre-immune serum followed by a 15nm gold-labeled goat anti-rabbit antibody. As observed in this image, no specific labeling can be observed within some of the major spore structures including the polar sac (PS), anchoring disk (AD), polar tube (PT), plasma membrane (PM), endospore (EN), and exospore (EX). Also, no specific labeling was observed within the host cell or within other stages of spore development (data not shown).

Immunolabeling with anti-rMADAM-His-Tag antibodies demonstrates that MADAM is localized to the polar sac-anchoring disk complex of mature *E. cuniculi* and *E. intestinalis* spores (Figures 19 and 20). The polar sac-anchoring disc complex is a bell-shaped structure located at the spore apex where the spore wall is thin (Wittner 1999). The polar sac is a vesicular structure composed of an electron-dense substance surrounded by a unit membrane (Wittner 1999). The polar sac encircles the proximal portion of the polaroplast. The polar tube enters the polar sac and terminates at a biconvex, layered structure known as the anchoring disk (Wittner 1999). The polar sac-anchoring disk complex serves as an anchor between the polar tube and spore wall during polar tube extrusion. By immunoelectron microscopy, MADAM appears to localize to the anchoring disk more often than the polar sac.

In addition to being localized to the polar sac-anchoring disk complex, MADAM can be found in the exospore and plasma membrane of *E. intestinalis* spores (Figure 20). In *E. cuniculi*, MADAM is only localized to the polar sac-anchoring disk complex (Figure 19). The exospore is the electron-dense, surface exposed layer of the microsporidia spore wall (Wittner 1999). In the spore wall, the plasma membrane lines the internal surface of the endospore (Wittner 1999). A difference in MADAM localization between *E. cuniculi* and *E. intestinalis* was unexpected and the relevance of this variation should be examined further.

Expression of MADAM appears to be developmentally or differentially regulated in *E. intestinalis* (Figure 20 and 21). During the meront to sporont transition, MADAM expression occurs internally and on the periphery (Figure 21). During sporoblast development, MADAM expression becomes more intense and delineated (Figure 21). In some spores, MADAM expression occurs on the plasma membrane while in other spores expression occurs on the exospore (Figure 20). Expression appears to be limited to one or the other location and

rarely does MADAM localize to both the exospore and plasma membrane within the same spore. Localization of MADAM to different structures within *E. intestinalis* spores may be an indication of spore maturity. Exospore localization occurs on spores that are forming an electron dense outer exospore layer (Figure 20). Localization of MADAM to the plasma membrane appears to occur in spores without this electron dense exospore layer (Figure 20).

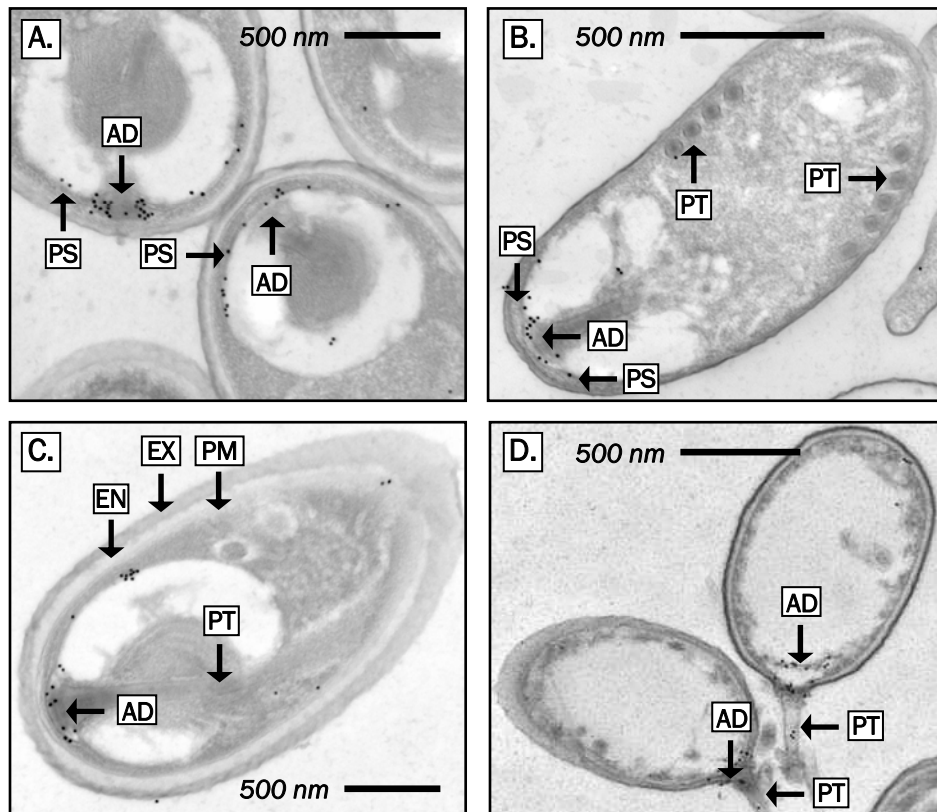


Figure 19 Localization of MADAM within *E. cucullis*. Sections of *E. cucullis* infected RK-13 cells were immunolabeled with antibodies against the rMADAM-His-Tag protein followed by a 15nm gold-labeled goat anti-rabbit antibody. (A-D) Immunolabeling is observed within the polar sac (PS) and anchoring disk (AD) of mature *E. cucullis* spores. (B-C) The polar tube (PT) emerges from the polar sac-anchoring disk complex. (C) No significant immunolabeling is observed in the exospore (EX) endospore (EN), or plasma membrane (PM) of the *E. cucullis* spores. (D) Immunolabeling is observed within the anchoring disk (AD) following polar tube extrusion.

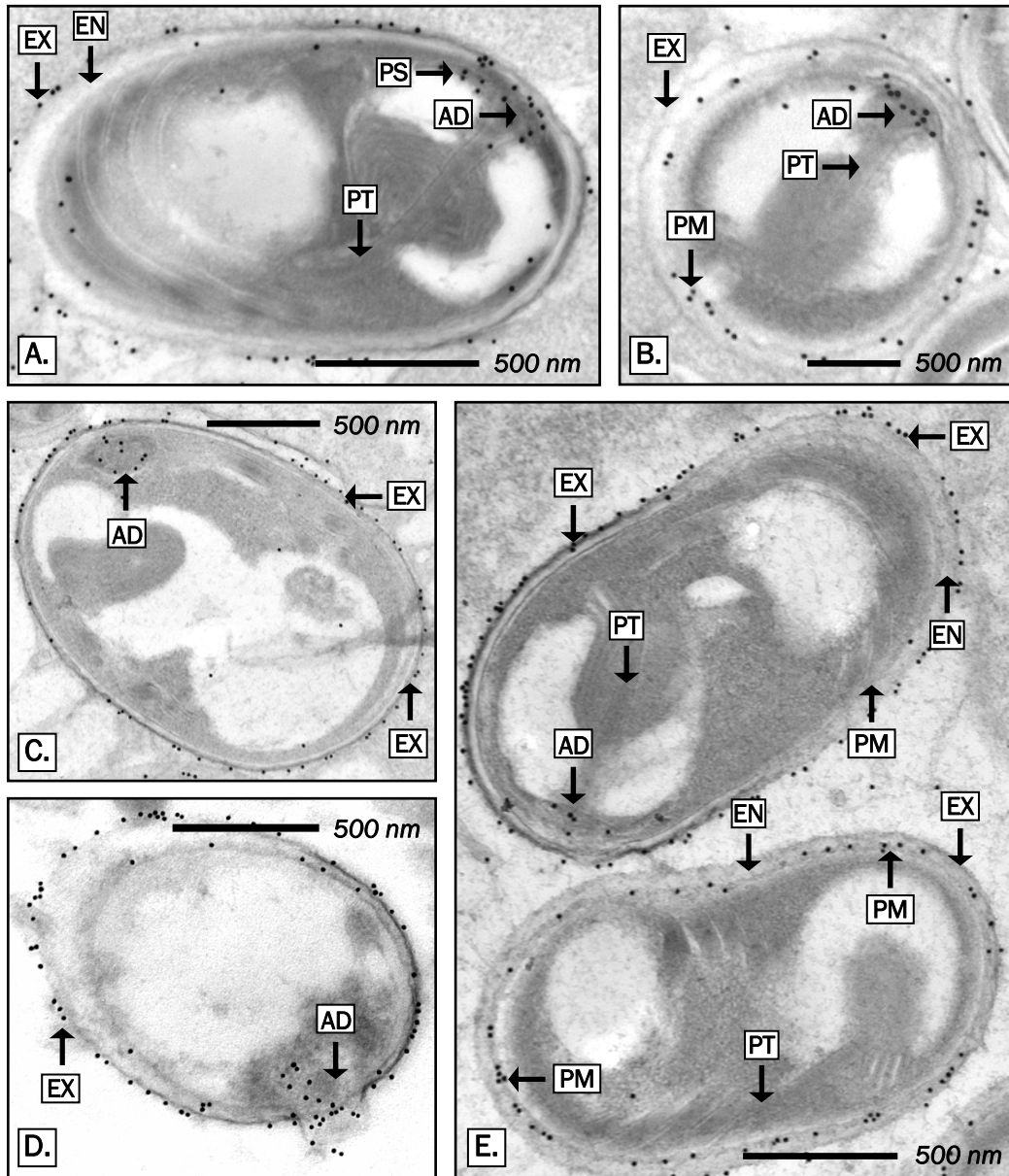


Figure 20 Localization of MADAM within *E. intestinalis*. Sections of *E. intestinalis* infected RK-13 cells were immunolabeled with antibodies against the rMADAM-His-Tag protein followed by a 15nm gold-labeled goat anti-rabbit antibody. (A-E) Immunolabeling is observed within the polar sac (PS) and anchoring disk (AD) of mature *E. intestinalis* spores. In contrast to *E. cuniculi*, localization of MADAM is also observed within the plasma membrane (PM) and exospore (EX) of *E. intestinalis*. MADAM does not appear within the endospore (EN). (A-B) The polar tube (PT) emerges from the polar sac-anchoring disk complex. (D) Immunolabeling of an *E. intestinalis* spore that has extruded its polar tube. (E) In the upper spore, MADAM is primarily located on the exospore (EX). In the lower spore, MADAM is primarily located on the plasma membrane (PM). Typically, MADAM does not localize to both the exospore and plasma membrane within the same spore.

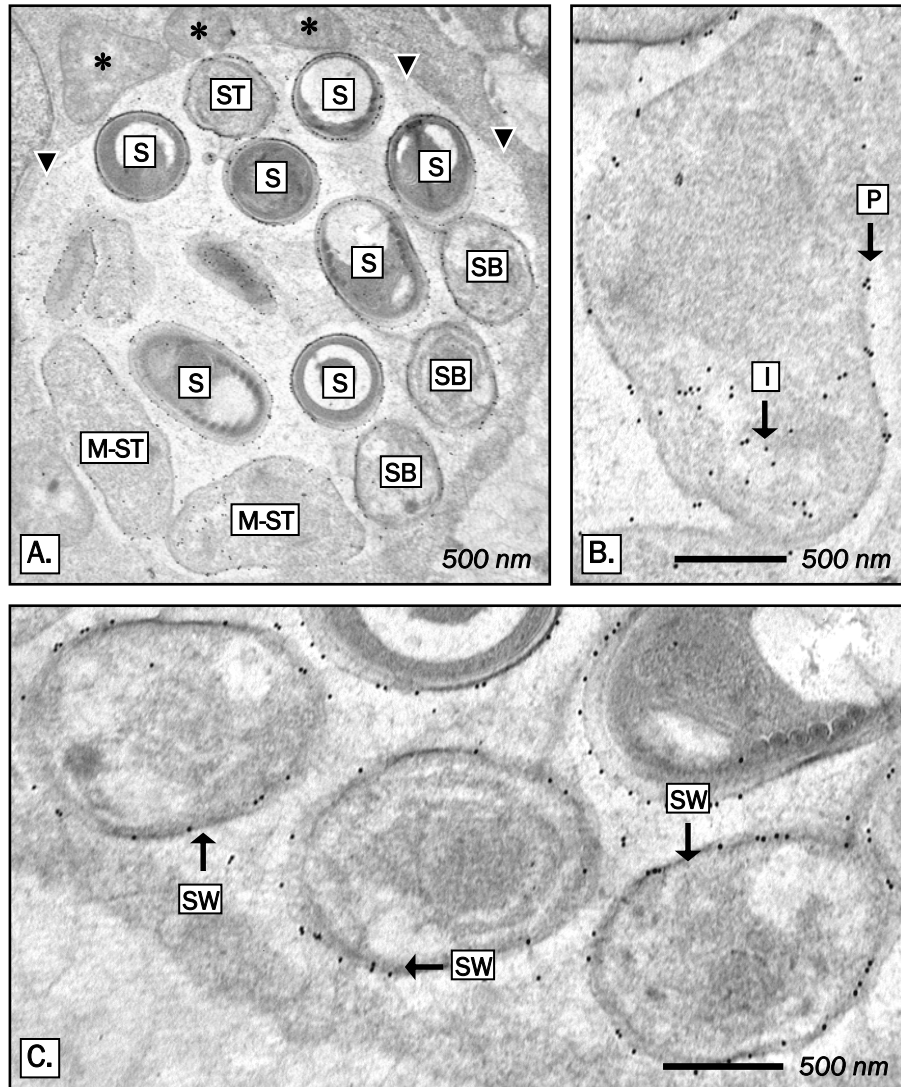


Figure 21 Localization of MADAM within various stages of *E. intestinalis* development. Sections of *E. intestinalis* infected RK-13 cells were immunolabeled with antibodies against the rMADAM-His-Tag protein followed by a 15nm gold-labeled goat anti-rabbit antibody. **(A)** Various developmental stages including the meront to sporont transition (M-ST), sporoblasts (SB), and spores (S) are observed within the parasitophorous vacuole (arrow-heads). In this image, host cell mitochondria (*) can be observed lining the outside of the parasitophorous vacuole. **(B)** During the transition between the meront and sporont, immunolabeling is observed internally (I) and along the periphery (P). **(C)** As development progresses from sporonts to sporoblasts (SB), immunolabeling is more concentrated along what will become the spore wall (SW).

Spore Adherence and Host Cell Infectivity Assays

A series of *in vitro* assays were performed to determine if rMADAM-His-Tag protein can be used to manipulate microsporidia spore adherence and/or host cell infection. In addition to the original rMADAM-His-Tag protein, other recombinant MADAM deletion mutants were also evaluated (Figure 22). rMET-His-Tag protein consists of the MADAM metalloprotease domain while the rPRO-His-Tag protein consists of the MADAM pro-domain. Although the disintegrin domain would be the most likely MADAM domain involved in adherence, our attempts to express the disintegrin domain alone were unsuccessful.

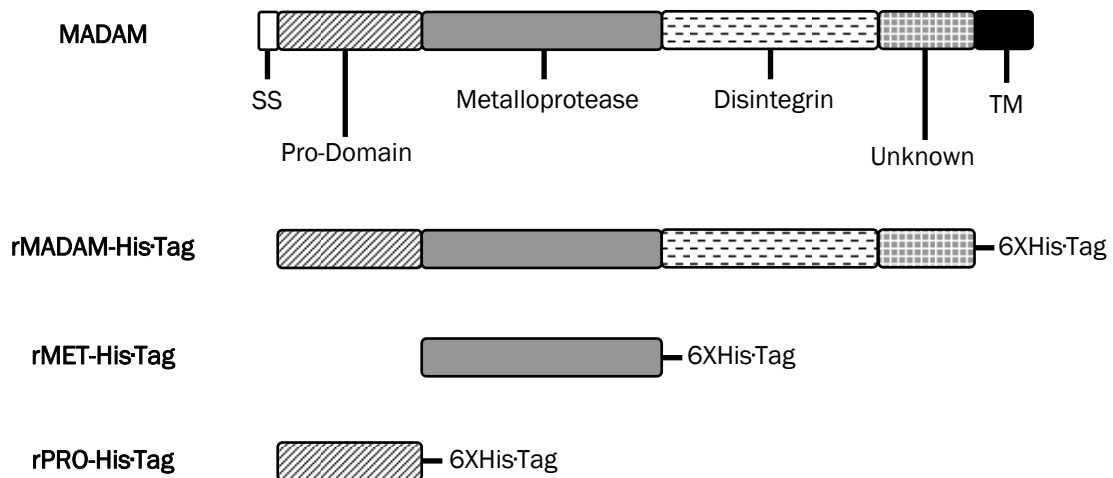


Figure 22 MADAM constructs introduced into the pET-21a vector. The domains of full-length MADAM protein are shown first followed by the deletion mutants constructed for insertion into the pET-21a vector. rMADAM-His-Tag does not have the signal sequence (SS) or transmembrane domain (TM). rMET-His-Tag consists of only the MADAM metalloprotease domain. rPRO-His-Tag consists of only the MADAM pro-domain. Attempts to express only the MADAM disintegrin domain were unsuccessful. The deletion mutants were generated in order to better characterize which domain or domains may be involved in spore adherence or host cell infection.

rMADAM-His-Tag protein was unable to significantly inhibit *E. cuniculi* spore adherence to the host cell monolayer (Figure 23). However, rMADAM-His-Tag protein inhibited *E. intestinalis* spore adherence to the host cell monolayer by 50-80% (Figure 23).

Addition of rMET-His-Tag or rPRO-His-Tag protein did not result in significant inhibition of *E. intestinalis* spore adherence to the host cell monolayer (Figure 23). The ability of rMADAM-His-Tag protein to inhibit *E. intestinalis* spore adherence but not *E. cuniculi* spore adherence could be related to the differences in MADAM localization between the two species. As stated previously, MADAM is localized on the surface exposed exospore of *E. intestinalis* but not *E. cuniculi*.

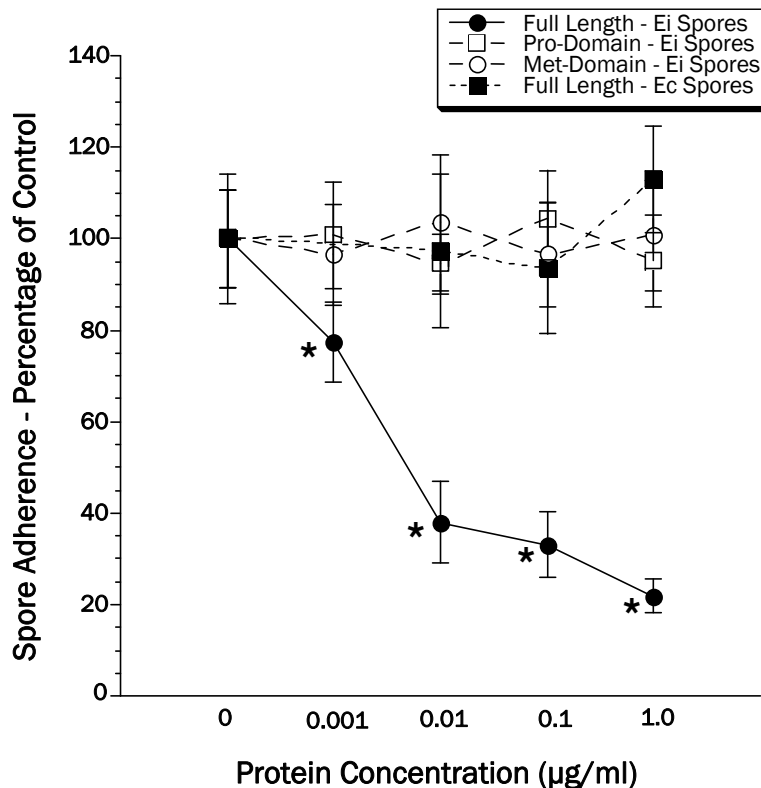


Figure 23 Analysis of spore adherence in the presence of recombinant MADAM proteins. Various dilutions of each recombinant protein were incubated on the host cell monolayers in the presence of *E. cuniculi* (Ec) or *E. intestinalis* (Ei) spores. Following an incubation period, the monolayers were washed to remove unbound spores. The host cell monolayers and bound spores were processed by indirect immunofluorescence methods. The number of adherent spores was determined and the data from three independent experiments are represented. Significance was determined using the Student's t-test and p-values less than 0.0001 are shown (*). rMADAM-His-Tag protein does not significantly inhibit *E. cuniculi* spore adherence (—■—) but does decrease *E. intestinalis* spore adherence (—●—) by as much as 80%. *E. intestinalis* spore adherence is not significantly decreased in the presence of recombinant protein consisting of the MADAM pro-domain (—□—) or MADAM metalloprotease domain (—○—).

Host cell infectivity assays revealed that rMADAM-His-Tag protein only decreased the occurrence of host cell infection by less than 20% (Figure 24). This result is unexpected given that the rMADAM-His-Tag protein decreases *E. intestinalis* spore adherence by 50%-80%. As a control, spore adherence and host cell infectivity assays using chondroitin sulfate A (CSA) were included. CSA decreased *E. intestinalis* spore adherence and host cell infection by at least 40%.

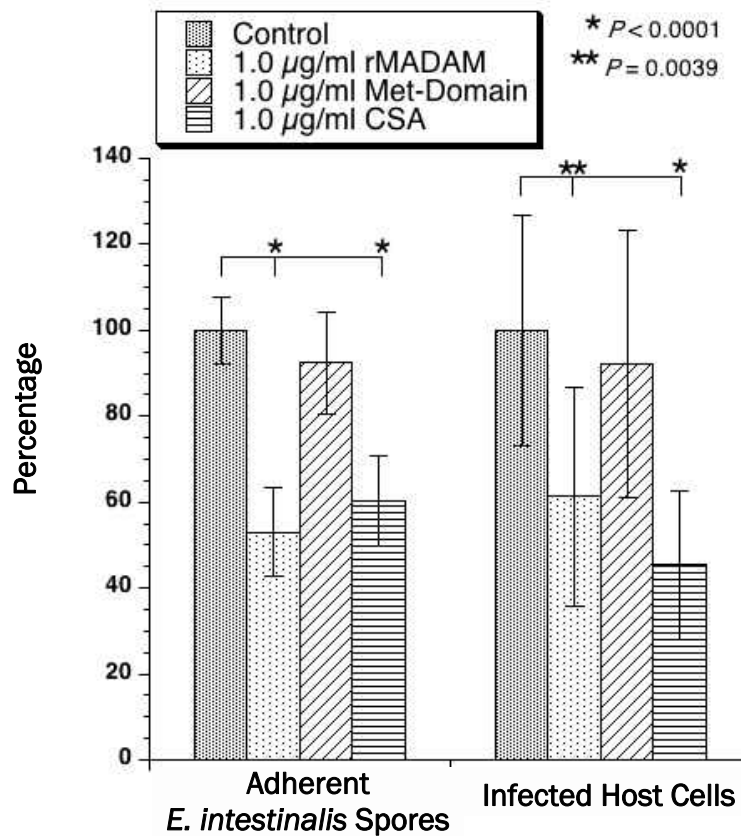


Figure 24 Analysis of host cell infection in the presence of recombinant MADAM proteins. Various dilutions of each recombinant protein were incubated on the host cell monolayers in the presence of *E. intestinalis* spores. Following an incubation period, the monolayers were washed to remove unbound spores and returned to tissue culture for several days. The host cell monolayers were washed, fixed, and stained with Uvitex 2B. The number of infected and non-infected host cells per field was determined. Duplicate monolayers were processed for spore adherence assays. Significance was determined using the Student's t-test and p-values less than 0.0001 (*) and equal to 0.0039 (**) are shown. rMADAM-His-Tag protein (▤) inhibited *E. intestinalis* spore adherence by ~50% but only decreased the percentage of infected host cells by ~20%. Chondroitin sulfate A or CSA (▥) was used as a positive control and was able to decrease *E. intestinalis* spore adherence and host cell infection by at least 40%.

Identification of Potential Protein-Protein Interactions Involving MADAM

As a protein sharing sequence homology with members of the ADAM family, it is possible that the MADAM protein serves several functions. To better understand what role MADAM serves, it is necessary to identify potential substrates or binding partners. MADAM has the potential to interact with numerous host cell and/or microsporidia proteins. A yeast two-hybrid approach was used to identify such protein-protein interactions involving MADAM.

A pGBKT7+MADAM (Δ SS/ Δ TM) plasmid encoding for a GAL4 DNA-BD+MADAM (Δ SS/ Δ TM) fusion protein was generated and transformed into AH109 yeast. Several yeast colonies (>100) grew on medium lacking tryptophan (SD/-Trp), which indicates that the transformants contain the pGBKT7+MADAM (Δ SS/ Δ TM) plasmid. The GAL4 DNA-BD+MADAM (Δ SS/ Δ TM) fusion protein was evaluated for transcriptional auto-activation and toxicity to the yeast cells. First, SD/-Trp/-His and SD/-Trp/-Ade medium were used to determine if the yeast transformants were capable of activating the *HIS3* and *ADE2* reporter genes. Yeast containing the pGBKT7+MADAM (Δ SS/ Δ TM) plasmid did not grow in the absence of adenine or histidine, indicating that the GAL4 DNA-BD+MADAM (Δ SS/ Δ TM) fusion protein could not activate transcription of the reporter genes. In addition, toxicity of the GAL4 DNA-BD+MADAM (Δ SS/ Δ TM) fusion protein was evaluated by comparing the growth rate of yeast containing the pGBKT7-MADAM (Δ SS/ Δ TM) plasmid and yeast containing the “empty” pGBKT7 vector. Yeast containing the pGBKT7+MADAM (Δ SS/ Δ TM) plasmid grew just as well as yeast containing the “empty” pGBKT7 vector. These data indicate that the pGBKT7+MADAM (Δ SS/ Δ TM) plasmid is suitable for yeast two-hybrid analysis.

A cDNA library was generated using the Matchmaker™ Library Construction and Screening Kit and RNA isolated from *E. intestinalis*-infected Vero cells. The GAL4 AD+cDNA

insert plasmids were generated by transforming the pGADT7-Rec vector and cDNA into the yeast simultaneously. In addition, these yeast were already contained the pGBKT7+MADAM (Δ SS/ Δ TM) plasmid. The yeast transformants were evaluated for growth on SD/-Leu/-Trp and SD/-Leu/-Trp/-His or TDO medium. Growth of the AH109 yeast on medium lacking tryptophan and leucine would indicate that the transformants contain the pGBKT7+MADAM (Δ SS/ Δ TM) plasmid and at least one pGADT7-Rec+cDNA insert plasmid. Yeast transformants growing on TDO medium would indicate a positive interaction between the GAL4 DNA-BD+MADAM (Δ SS/ Δ TM) fusion protein and a GAL4 AD+cDNA fusion protein. Over 1,000 colonies grew on the SD/-Leu/-Trp medium. Over a period of several days, 89 yeast colonies grew on the TDO medium. All of the 89 yeast colonies were transferred to fresh TDO medium and QDO (SD/-Leu/-Trp/-His/-Ade) medium to screen for stringency of the interactions.

To identify the cDNA from the positive yeast colony the cDNA insert must first be “rescued” by Plasmid Isolation or PCR Colony Screening. PCR Colony Screening was selected because it offers an efficient initial screening method. Isolating the plasmid from each positive yeast clone would have been more costly and time consuming. PCR amplifications of the cDNA insert from each yeast colony were separated by agarose gel electrophoresis (Figure 25). Fifty-six percent of the yeast colonies resulted in PCR products with multiple DNA bands.

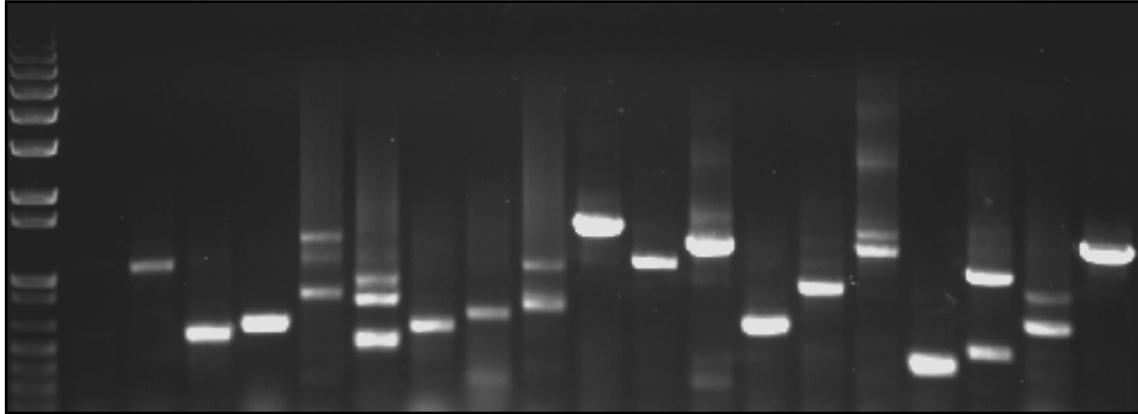


Figure 25 Amplification of cDNA inserts from potential positive yeast clones. cDNA inserts were amplified from a scraping of each yeast colony using primers specific for the pGADT7-Rec vector. PCR products were then separated by agarose gel electrophoresis. The DNA ladder can be observed in the far left lane followed by PCR bands representative of cDNA inserts. Some colonies possess more than one pGADT7-Rec vector as evident by the appearance of several PCR bands within a single sample. Although all 89 colonies were screened by PCR, this gel is only representative of eighteen of those colonies.

PCR products that appeared to be a single PCR band were purified and sent to the Molecular Biology Core Facility (East Tennessee State University; Johnson City, TN) for DNA sequencing. If the DNA sequence was usable, then the in-frame DNA sequence corresponding to the cDNA insert was translated to the appropriate protein sequence using ExPASy's Translate Tool (Gasteiger and others 2003). The translated protein sequence was analyzed using the Basic Local Alignment Tool (BLAST) to determine the protein identification (Altschul and others 1990). Protein identifications from sequenced cDNA inserts were compiled and examined for evidence of potential false-positive interactions (Table 3).

Table 3 Basic Local Alignment Tool (BLAST) identification of PCR amplified cDNA inserts from yeast colonies demonstrating potential interactions involving the MADAM (Δ SS/ Δ TM) protein. *

Colony #	Protein	Organism	NCBI Identification	E-Value	Growth on QDO
2	serine/threonine protein kinase	<i>Rattus norvegicus</i>	NP_775449.1	8×10^{-4}	✓
3	leucine rich repeat containing 22	<i>Homo sapiens</i>	NP_001017924	5×10^{-7}	✓
4	No similarity found	_____	_____	_____	✓
7	similar to hornerin	<i>Homo sapiens</i>	XP_001127437	0.11	✓
8	No similarity found	_____	_____	_____	x
10	unnamed protein product	<i>Homo sapiens</i>	BAC87430	0.7	✓
11	unreadable sequence data	_____	_____	_____	✓
12	unreadable sequence data	_____	_____	_____	✓
13	unreadable sequence data	_____	_____	_____	✓
14	No similarity found	_____	_____	_____	x
16	unreadable sequence data	_____	_____	_____	✓
19	No similarity found	_____	_____	_____	x
22	methionine aminopeptidase 2	<i>E. intestinalis</i>	AAR04555	2×10^{-69}	✓
23	unreadable sequence data	_____	_____	_____	✓
25	No similarity found	_____	_____	_____	✓
29	NAD-dependent epimerase	<i>Roseiflexus sp.</i>	ZP_01355602	1.7	✓
30	No similarity found	_____	_____	_____	✓
31	No similarity found	_____	_____	_____	✓
32	No similarity found	_____	_____	_____	✓

Colony #	Protein	Organism	NCBI Identification	E-Value	Growth on QDO
33	histone H3	<i>E. cuniculi</i>	NP_597654	6×10^{-55}	x
34	histone H3	<i>E. cuniculi</i>	NP_597654	6×10^{-57}	x
35	no similarity found	_____	_____	_____	x
37	no similarity found	_____	_____	_____	x
40	polar tube protein 3 precursor	<i>E. cuniculi</i>	Q8MTP3	4×10^{-104}	✓
42	unreadable sequence data	_____	_____	_____	✓
46	GATA zinc finger transcription factor	<i>E. cuniculi</i>	NP_584553		x
50	unreadable sequence data	_____	_____	_____	✓
56	polar tube protein 3 precursor	<i>E. cuniculi</i>	Q8MTP3	2×10^{-9}	✓
61	polar tube protein 3 precursor	<i>E. cuniculi</i>	Q8MTP3	7×10^{-69}	✓
62	no similarity found	_____	_____	_____	✓
64	unnamed protein product	<i>Homo sapiens</i>	BAC85628	2×10^{-23}	✓
67	unreadable sequence data	_____	_____	_____	✓
68	unreadable sequence data	_____	_____	_____	✓
69	no similarity found	_____	_____	_____	✓
70	hypothetical protein ORF501	<i>Costesia plutellae</i>	AAZ04273	0.19	✓
71	hypothetical protein ECU07_1800	<i>E. cuniculi</i>	NP_586107	0.059	✓
76	unreadable sequence data	_____	_____	_____	✓
77	no similarity found	_____	_____	_____	✓

Colony #	Protein	Organism	NCBI Identification	E-Value	Growth on QDO
79	unreadable sequence data	_____	_____	_____	✗
81	no similarity found	_____	_____	_____	✓
82	no similarity found	_____	_____	_____	✓
84	unreadable sequence data	_____	_____	_____	✓
86	Macrophage migration inhibitory factor	<i>Homo sapiens</i>	CAG46452	1×10^{-28}	✓
88	unreadable sequence data	_____	_____	_____	✓
89	unreadable sequence data	_____	_____	_____	✓

* PCR products from 45 of the original 89 positive yeast transformants were sent for sequencing analysis. 31% of the DNA sequences were unusable and another 33% of them resulted in no protein identification. We were able to obtain protein identifications from the remaining DNA sequences. BLAST results with E-values approaching 1.0 are not considered to be reliable. Yeast colonies that do not grow on QDO medium (✗) represent either false-positives or true protein-protein interactions that are weak. Yeast colonies that do grow on QDO medium (✓) are considered to be strong protein-protein interactions.

Fifteen of the 45 PCR products resulted in a sequence without homology to any protein in the NCBI database and are listed as “no similarity found” (Table 3). These PCR products are a consequence of pGBKT7-Rec+cDNA plasmids with cDNA inserts that are apparently out-of-frame. Yeast transformed with out-of-frame pGBKT7-Rec+cDNA plasmids can yield a positive interaction by producing short peptides that interact with the GAL4 DNA-BD fusion protein but do not represent a biologically relevant interaction. These yeast two-hybrid interactions are considered to be false-positives (Vidalain and others 2004).

Fourteen of the 45 PCR products resulted in an unreadable DNA sequence. A chromatogram was classified as unreadable or unusable in cases where the sequence corresponding to the cDNA insert consisted of single nucleotide tracts (Figure 26), “mixed peaks”, or areas of poor resolution. PCR products that appear as a single DNA band may consist of additional DNA bands that do not appear on the agarose gel because they are too small or are superimposed products.

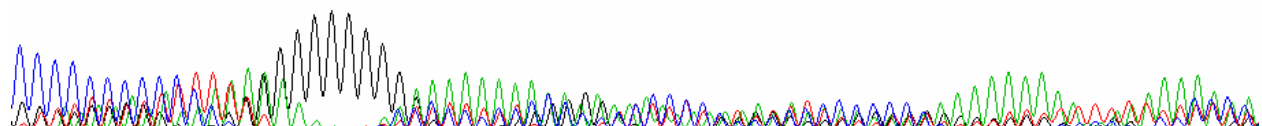
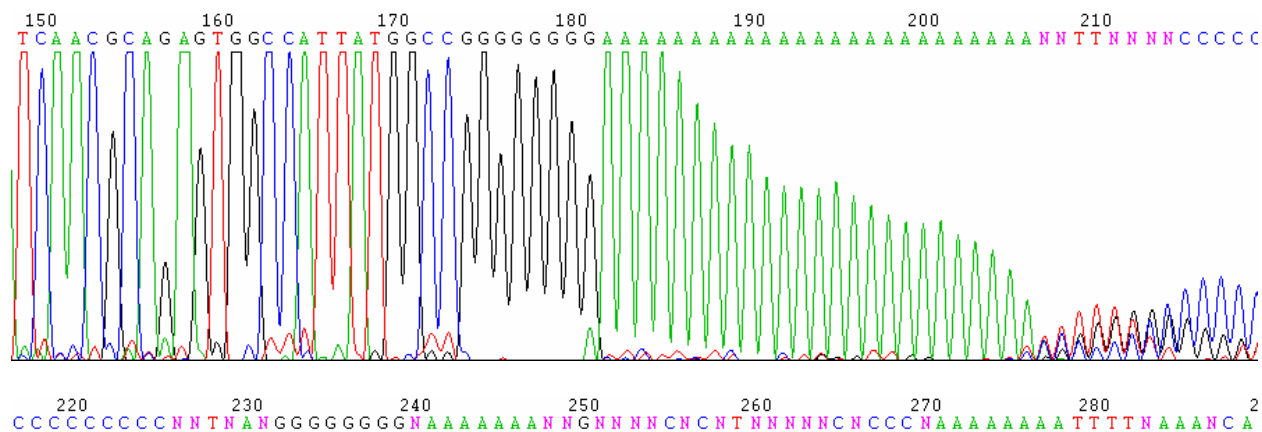


Figure 26 Chromatogram demonstrating an unreadable DNA sequence. Some PCR products that appeared to consist of a single band were shown to possess other contaminating DNA products most likely from other cDNA inserts. All of the unreadable DNA sequences were not usable from the point at which the cDNA insert sequence should start. For this chromatogram it would have been around base 180.

There are at least two categories of false-positives: “biological” false-positives are defined as protein-protein interactions that occur in the yeast cell but do not occur in the organism under study and “technical” false-positives are protein-protein interactions that occur during a yeast-two hybrid screen due to the limitations of the system (Vidalain and others 2004). Although “biological” false-positives are difficult to eliminate, several of the “technical” false-positives can be avoided. One type of false-positive can arise due to the ability of a yeast cell to stably maintain more than one plasmid. Yeast two-hybrid screening can lead to a yeast cell transformed with multiple pGADT7-Rec+cDNA plasmids. Screening of our positive yeast colonies revealed that 56% of the transformants actually contained

multiple pGADT7-Rec+cDNA plasmids as evident by the appearance of multiple PCR products from a single colony.

In an attempt to select for the correct plasmid, all of the yeast transformants were grown under positive selection pressure by replica plating on TDO medium every 3 days for 15 days as previously described (Vidalain and others 2004). After replica plating the yeast were PCR screened again to determine if any had lost potential contaminating pGADT7-Rec+cDNA plasmids. First, colonies #1-38 were PCR screened and 18 of the colonies appeared to lose their contaminating plasmids. However, several of these PCR products were again sent for sequencing and several still did not result in a usable DNA sequence. Attempts to purify individual PCR bands from the agarose gel for sequencing also did not increase the quality of the DNA sequence. Future attempts to identify the cDNA inserts will be done by isolating individual plasmids from the yeast colonies for sequence analysis.

Examination of the usable sequence data, revealed 16 potential protein identifications. At least 6 of these sequences (colony #2, 7, 10, 29, 70, and 71) led to BLAST results with e-values approaching 1.0, which indicates that the quality of the DNA sequence may not be high enough to reliably identify the cDNA insert (Vidalain and others 2004). In addition, at least 3 sequences (colony #33, 34, and 46) led to the identification of proteins that may result in false-positive interactions because they are inherently “sticky” and are commonly classified as generating false-positive interactions during yeast two-hybrid analysis (Table 4).

Table 4 Proteins commonly identified as false-positives during yeast two-hybrid analysis. (adapted from Vidalain and others 2004).

Protein	Number of Times Found as False-Positive
heat shock proteins	16
ribosomal proteins	14
cytochrome oxidase	5
proteasome subunits	4
Ferritin	4
other mitochondrial proteins	3
transfer-RNA synthase	3
collagen-related proteins	3
zinc-finger containing proteins	3

After evaluating the cDNA insert data, we found methionine aminopeptidase 2 (MetAP2) and polar tube protein 3 (PTP3) to be the most interesting potential partners for the MADAM protein. MetAP2 is an essential participant in the N-terminal methionine excision pathway and is responsible for post-translational modification of nascent proteins by removing the N-terminal methionine (Upadhya and others 2006). Fumagillin, one of the therapies used for the treatment of human microsporidiosis, covalently binds to MetAP2 and specifically inhibits the peptidase activity. Although the potential interaction between MetAP2 and MADAM is worth characterizing further, we were more interested in investigating PTP3 protein. First, this cDNA insert was positively identified from sequencing data from 3 separate colonies #40, 56, and 61 (Table 3). PCR screening of colony #10, 31, 57, and 59 resulted in DNA bands the same size as the 3 other cDNA inserts that were identified as PTP3. These colonies were assumed to contain the PTP3 cDNA insert. In addition, a potential interaction between MADAM and PTP3 seems likely because MADAM is located in the polar sac-anchoring disk complex.

In situ analysis reveals that PTP3 is a slightly acidic protein (pI 6.47) of ~136kDa with a large acidic core flanked by highly basic N- and C-terminal domains (Peuvel and others 2002). PTP3 is much larger than the other two known polar tube proteins and does not contain any cysteine residues. Polyclonal antibodies generated against recombinant PTP3 protein (amino acids 141-574) were used to confirm the location of the PTP3 protein (Peuvel and others 2002). Immunofluorescence microscopy demonstrated that anti-rPTP3 antibodies specifically react with the extruded polar tube of *E. cuniculi* (Figure 27). In addition, immunoelectron microscopy demonstrated localization of PTP3 within cross-sections of the *E. cuniculi* polar tube (Figure 27).

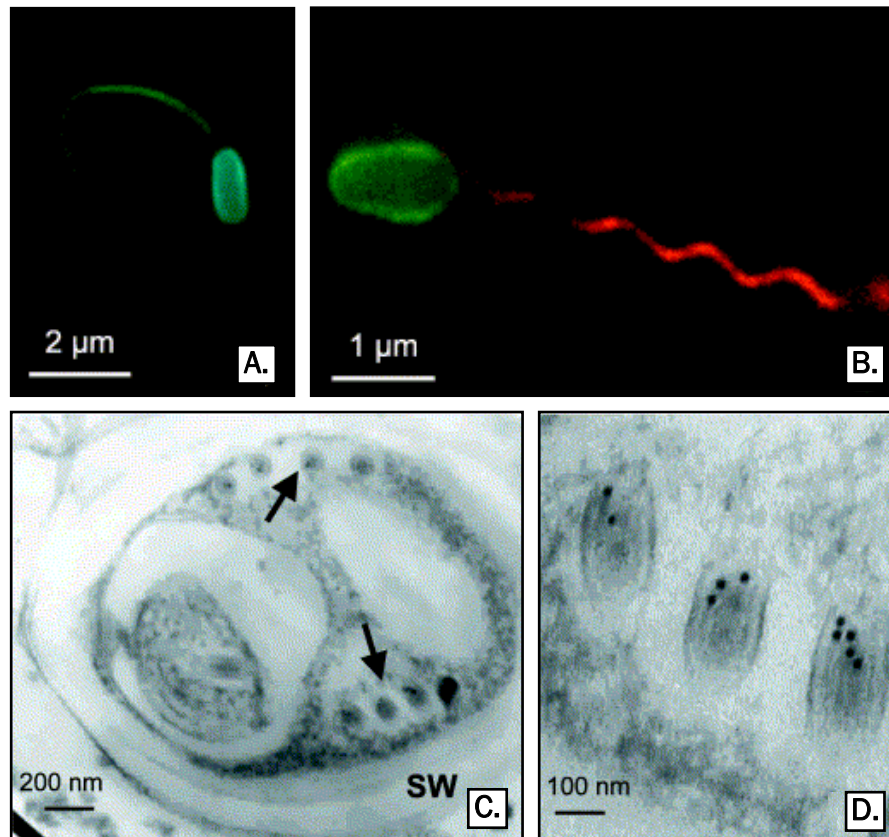


Figure 27 Localization of PTP3 within *E. cuniculi*. Immunolocalization of PTP3 using antibodies generated against recombinant PTP3 (amino acid 141-574). **(A)** An *E. cuniculi* spore (blue fluorescence) with its polar tube (green fluorescence) extruded was labeled with a 1:100 dilution of the anti-rPTP3 antibody (green fluorescence) and Uvitex 2B (blue fluorescence). **(B)** Dual immunolabeling using anti-rPTP3 with a TRITC-conjugated secondary antibody and a spore wall antiserum with a FITC-conjugated secondary antibody. The anti-rPTP3 antibody specifically reacts with the extruded polar tube (red fluorescence). **(C-D)** An *E. cuniculi* spore was labeled with anti-rPTP3 antibodies for immunoelectron microscopy. Notice the internal coiled polar tube (arrows). At a high magnification, the gold particles can be seen within the polar tube coils. The anti-rPTP3 antibodies do not react with the spore wall (SW). (adapted from Peuvrel and others 2002).

Peuvrel and others found that addition of a thiol cleavable cross-linking agent, DSP, to crude extracts of *E. cuniculi* spores led to the precipitation of a large protein complex. Cleavage of the cross-links and separation of the proteins by SDS-PAGE revealed a pattern of five major protein bands. PTP1 and PTP2 were the predominant components of the complex (Peuvrel and others 2002). The slowest migrating band was representative of PTP3. DSP mediated the formation of a large protein complex comprised of at least three proteins

derived from the *E. cuniculi* polar tube and two unidentified proteins. PTP3 lacks cysteine residues but is rich in charged residues and it has been suggested that PTP3 may interact with PTP1 and/or PTP2 via ionic bonds to aid in the formation of PTP1-PTP2 polymers during polar tube extrusion (Peuvel and others 2002).

To further characterize the potential interaction between MADAM and PTP3, additional yeast two-hybrid experiments were performed. First, amino acids 141-574 of *E. cuniculi* PTP3 were introduced into the pGADT7-Rec vector by homologous recombination. Yeast transformed with the pGBKT7+MADAM (Δ SS/ Δ TM) and the pGADT7-Rec+EcPTP3 plasmids were screened for a potential interaction. The yeast grew on SD/-Leu/-Trp medium indicating that the transformants contain the pGBKT7+MADAM (Δ SS/ Δ TM) vector and the pGADT7-Rec+EcPTP3 vector. In addition, several of the yeast transformants grew on TDO medium which indicates a potential positive interaction between the GAL4 DNA-BD+MADAM (Δ SS/ Δ TM) fusion protein and the GAL4 AD+EcPTP3 fusion protein (Figure 28 and Figure 29). As expected, yeast transformed with only the pGADT7-Rec+EcPTP3 plasmid only grew on SD/-Leu medium (data not shown). These initial yeast two-hybrid experiments indicate that MADAM has the ability to interact with PTP3 from *E. cuniculi* and *E. intestinalis*.

To more specifically identify which MADAM domain or domains are responsible for the potential interaction with PTP3, several MADAM deletion mutants were generated and evaluated. An overnight culture from each yeast colony was prepared and the OD₆₀₀ of each culture was normalized prior to plating a dilution series on DDO, TDO, and QDO medium. Deletion of the unknown region alone (Δ SS/ Δ UNK/ Δ TM) or in combination with the disintegrin domain (Δ SS/ Δ DIS/ Δ UNK/ Δ TM) did not appear to decrease the interaction between MADAM and EiPTP3 (Figure 30). However, deletion of the disintegrin domain in

combination with the unknown region (MADAM Δ SS/ Δ DIS/ Δ UNK/ Δ TM) did appear to slightly decrease the ability of MADAM to interact with EcPTP3 (Figure 29). The ability of MADAM to interact with EcPTP3 and EiPTP3 was almost completely eliminated upon removal of the metalloprotease domain (Δ SS/ Δ MET/ Δ TM) from the MADAM construct (Figure 29 and 30). Our yeast two-hybrid analyses at least indirectly indicate that the interaction between MADAM and PTP3 relies on the MADAM metalloprotease domain. Additional yeast two-hybrid analyses should be conducted using a MADAM construct that consists of a mutated metalloprotease catalytic site instead of a complete deletion of the metalloprotease domain.

Yeast two-hybrid screens were also performed to determine if MADAM interacts with either PTP1 or PTP2. According to the yeast two-hybrid data, MADAM appears to interact with both EcPTP1 and EcPTP2 but does not interact with EcPTP2 as strongly as it does with EcPTP1 or EcPTP3 (Figure 28 and Figure 29). Yeast transformants containing the pGADT7-Rec+EcPTP2 and pGBKT7+MADAM (Δ SS/ Δ TM) plasmids do not grow on the most stringent medium (QDO) whereas those with the pGADT7-Rec+EcPTP1 plasmid or pGADT7-Rec+EcPTP3 plasmid do. Interestingly, MADAM does not interact with EiPTP1 as strongly as it does with EiPTP2 or EiPTP3 (Figure 30).

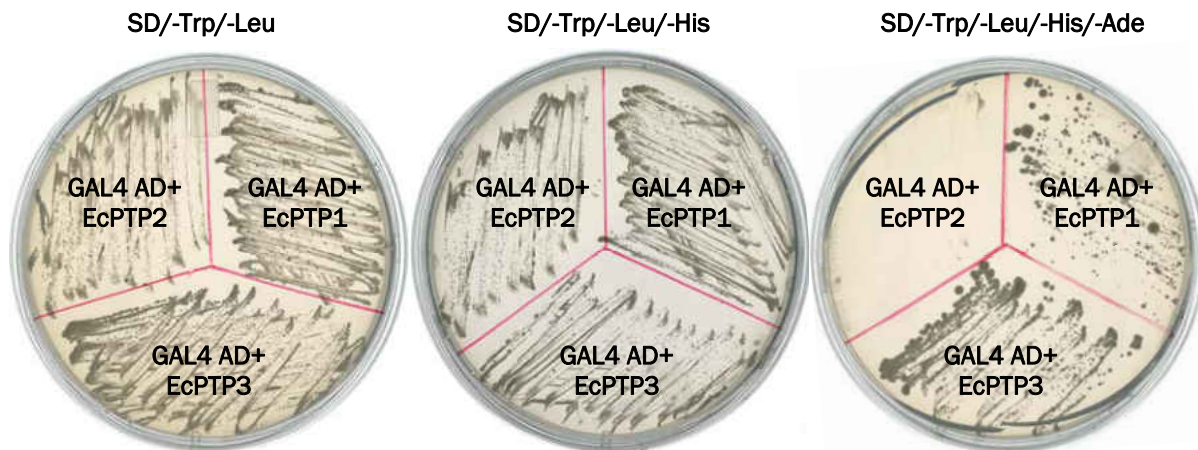


Figure 28 Yeast two-hybrid analysis of GAL4 DNA-BD+MADAM (Δ SS/ Δ TM) and GAL4 AD+*E. cuniculi* polar tube protein 1, 2, and 3. First, the yeast were transformed with the vector to express the GAL4 DNA-BD+MADAM (Δ SS/ Δ TM) fusion protein. The yeast were then transformed with vectors to express GAL4 AD-EcPTP1, EcPTP2, or EcPTP3 fusion proteins. A yeast colony representative of each transformant was re-streaked onto selective medium for evaluation of reporter gene expression. Growth of the yeast on SD/-Trp/-Leu medium indicates that both vectors are present. Growth of the yeast on SD/-Trp/-Leu/-His medium indicates that an interaction is occurring between the fusion proteins. A higher level of selection is provided by analyzing the yeast for growth on the SD/-Trp/-Leu/-His/-Ade medium. MADAM appears to interact with EcPTP1, EcPTP2, and EcPTP3 as evident by the growth of the yeast on the SD/-Trp/-Leu/-His medium. The interaction between MADAM and EcPTP1 and EcPTP3 is stronger than the interaction between MADAM and EcPTP2. Yeast expressing the GAL4 DNA-BD+MADAM (Δ SS/ Δ TM) fusion protein and the GAL4 AD-EcPTP2 fusion protein does not grow on the SD/-Trp/-Leu/-His/-Ade medium.

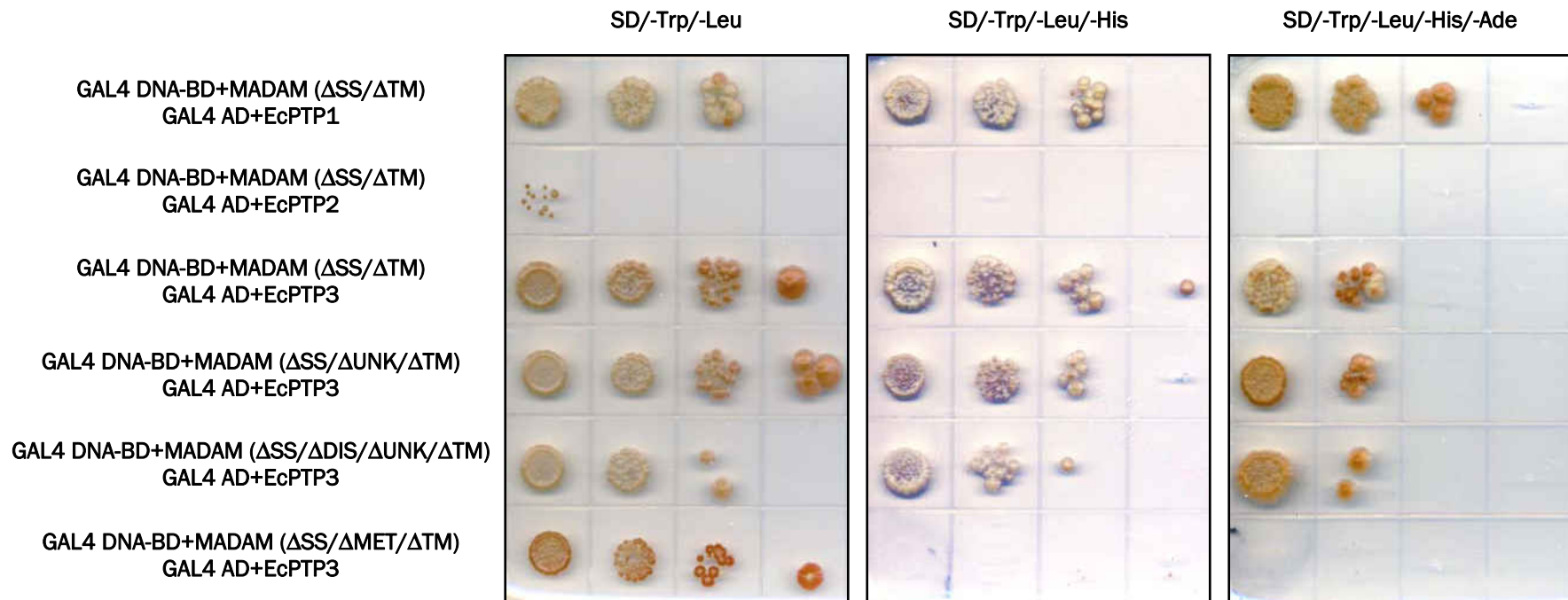


Figure 29 Yeast two-hybrid analysis of MADAM and the *E. cuniculi* polar tube proteins. First, yeast were transformed with vectors to express various GAL4 DNA-BD+MADAM fusion proteins. The yeast were then transformed with vectors to express GAL4 AD-EcPTP1, EcPTP2, or EcPTP3 fusion proteins. Serial dilutions from normalized overnight yeast cultures were evaluated for growth on selective medium. Growth of the yeast on SD/-Trp/-Leu medium indicates that both vectors are present. Growth of the yeast on SD/-Trp/-Leu/-His medium indicates that an interaction is occurring between the fusion proteins. A higher level of selection is provided by analyzing the yeast for growth on the SD/-Trp/-Leu/-His/-Ade medium. MADAM appears to interact with EcPTP1, EcPTP2, and EcPTP3. The interaction between MADAM and EcPTP1 and EcPTP3 is stronger than the interaction between MADAM and EcPTP2. During preparation of the dilution series, the yeast colony expressing GAL4 DNA-BD+MADAM (Δ SS/ Δ TM) and GAL4 AD+EcPTP2 did not grow as expected as evident by the lack of growth on SD/-Trp/-Leu medium. However, this yeast colony has been streaked onto selective medium and they grow well on SD/-Trp/-Leu and SD/-Trp/-Leu/-His but not on SD/-Trp/-Leu/-His/-Ade (Figure 28). Evaluation of interactions between the MADAM deletion mutants and EcPTP3 revealed that removal of the metalloprotease domain was able to decrease the ability of the yeast to grow on the SD/-Trp/-Leu/-His and SD/-Trp/-Leu/-His/-Ade.

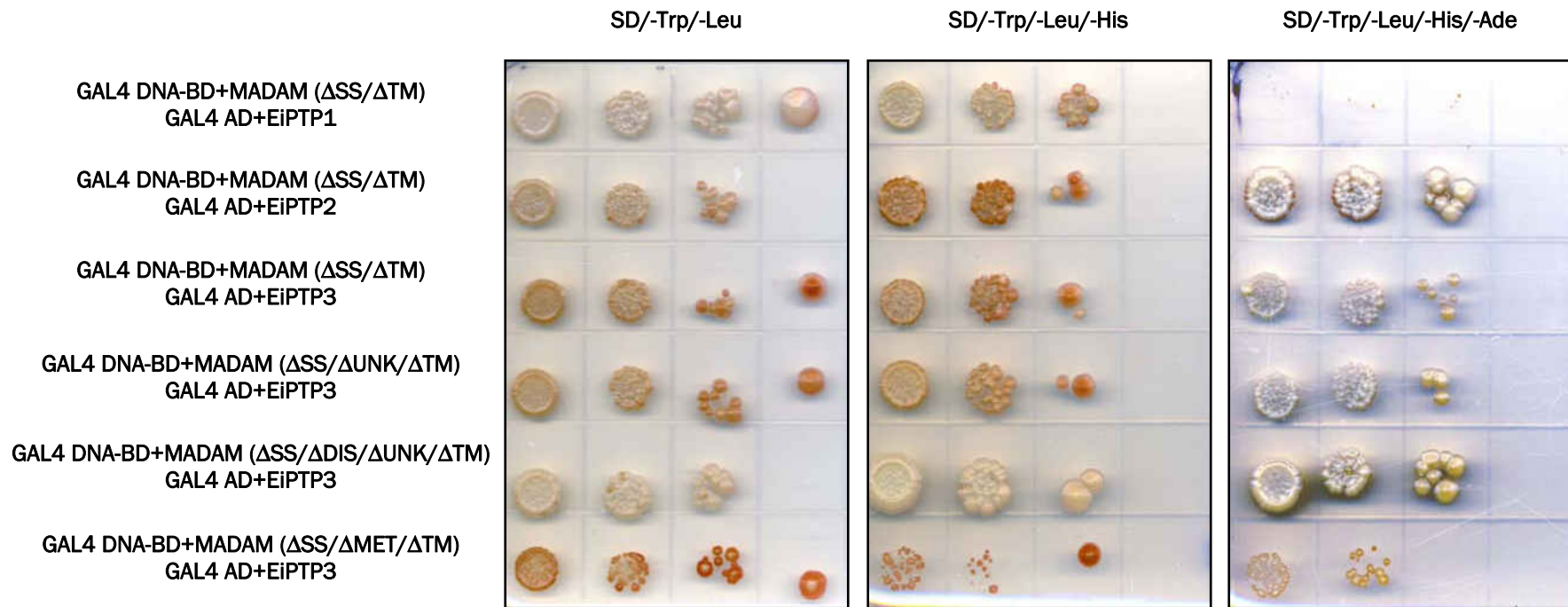


Figure 30 Yeast two-hybrid analysis of MADAM and the *E. intestinalis* polar tube proteins. First, yeast were transformed with vectors to express various GAL4 DNA-BD+MADAM fusion proteins. The yeast were then transformed with vectors to express GAL4 AD-EiPTP1, EiPTP2, or EiPTP3 fusion proteins. Serial dilutions from normalized overnight yeast cultures were evaluated for growth on selective medium. Growth of the yeast on SD/-Trp/-Leu medium indicates that both vectors are present. Growth of the yeast on SD/-Trp/-Leu/-His medium indicates that an interaction is occurring between the fusion proteins. A higher level of selection is provided by analyzing the yeast for growth on the SD/-Trp/-Leu/-His/-Ade medium. MADAM appears to interact with EiPTP1, EiPTP2, and EiPTP3. The interaction between MADAM and EiPTP2 or MADAM and EiPTP3 is stronger than the interaction between MADAM and EiPTP1. Evaluation of interactions between the MADAM deletion mutants and EiPTP3 revealed that removal of the disintegrin domain or unknown region does not appear to decrease the interaction between MADAM and EiPTP3. Unlike the interaction between MADAM and EcPTP3, removal of the metalloprotease domain only slightly decreased the interaction between MADAM and EiPTP3.

Confirmation of Yeast Two-Hybrid Interactions Using *In Vitro* Co-Immunoprecipitation

In vitro co-immunoprecipitation is a popular technique used to confirm protein-protein interactions initially identified during yeast two-hybrid screening. *In vitro* transcription and translation procedures were performed using the pGBKT7+MADAM (Δ SS/ Δ TM), pGADT7-Rec+EcPTP2, and pGADT7-Rec+EcPTP3 vectors to generate ^{35}S -labeled c-Myc+MADAM, HA+EcPTP2, and HA+EcPTP3 fusion proteins (Figure 31). During the co-immunoprecipitation studies, HA-Tag Polyclonal Antibody was able to immunoprecipitate an EcPTP2-MADAM and an EcPTP3-MADAM complex (Figure 31). We had anticipated that the interaction between MADAM and EcPTP2 may be too weak to detect by co-immunoprecipitation.

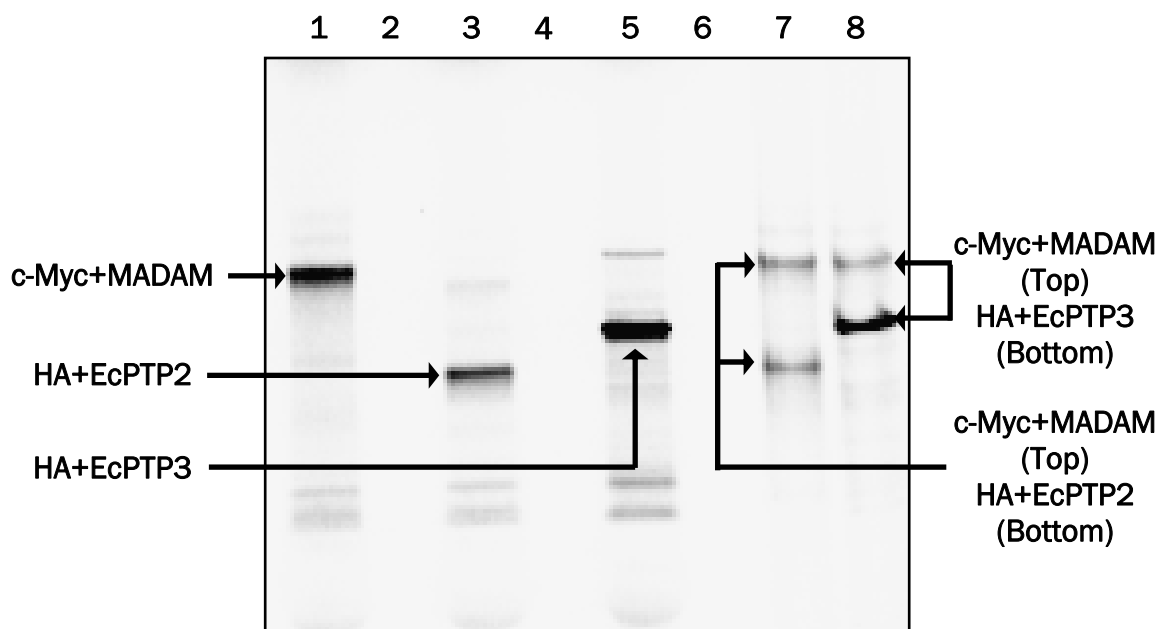


Figure 31 *In vitro* co-immunoprecipitation studies involving MADAM, EcPTP2, and EcPTP3. ^{35}S -labeled c-Myc+MADAM (Lane 1), HA+EcPTP2 (Lane 3), and HA+EcPTP3 (Lane 5) proteins were generated using the PROTEINSCRIPT® II *in vitro* transcription and translation protocol. c-Myc +MADAM and HA+EcPTP2 complexes (Lane 7) as well as c-Myc+MADAM and HA+EcPTP3 complexes (Lane 8) were immunoprecipitated in the presence of the anti-HA antibody. Each protein sample was separated by SDS-PAGE and analyzed by autoradiography. The c-Myc+MADAM protein should be ~59kDa. The HA+EcPTP2 protein should be ~35kDa. The HA+EcPTP3 protein should be ~51kDa.

CHAPTER 4

CONCLUSIONS

Since being recognized as a cause of chronic diarrhea in individuals infected with HIV, interest in microsporidia as human pathogens has grown. Treatments options for human microsporidiosis are limited and there is a pressing need for continued research to develop better therapeutic strategies. In addition to being pathogens of importance to human health, microsporidia also provide an opportunity to study the basic biology of highly specialized fungi. A particularly fascinating characteristic of all microsporidia is the possession of a unique invasion apparatus known as the polar tube. Traditionally, microsporidia were believed to infect host cells by extruding the polar tube at a velocity fast enough to pierce the host cell plasma membrane thereby allowing the infectious sporoplasm to pass through the hollow polar tube and into the host cell cytoplasm (Vivares and Metenier 2001). Many of the details regarding how polar tube extrusion leads to host cell infection are still undetermined.

Microsporidia spore adherence to the host cell surface is hypothesized to be a prerequisite to polar tube extrusion and subsequent host cell infection. Using an *in vitro* system *E. intestinalis* spores were shown to adhere to the host cell surface through at least one mechanism involving sulfated glycosaminoglycans (Hayman and others 2005). Numerous organisms including bacteria, viruses, and parasites exploit host cell glycosaminoglycans as adhesion receptors (Rostand and Esko 1997). By manipulating host cell glycosaminoglycans during microsporidia spore adherence, we were able to demonstrate that a decrease in spore adherence led to a decrease in the occurrence of host cell infection (Hayman and others 2005). These data represented the first evidence that

adherence of the microsporidia to the host cell surface directly correlates to host cell infection.

Further examination of the factors involved in microsporidia spore adherence revealed a potential role of divalent cations, which are known effectors of numerous host-pathogen interactions (Anzinger and others 2006; Southern and others 2006). Addition of exogenous manganese and magnesium to the tissue culture medium resulted in an increase in adherence of *E. cuniculi* and *E. intestinalis* spores to the host cell monolayer and a subsequent increase in host cell infection (Southern and others 2006). Interestingly, calcium did not contribute to an increase in microsporidia adherence but did lead to an increase in host cell infection (Southern and others 2006). Calcium, which is known to play a role in the swelling of the polaroplast during polar tube extrusion, was hypothesized to increase the occurrence of polar tube extrusion and subsequent host cell infection in our *in vitro* system. In support of this hypothesis, chelating agents were found to eliminate the augmentation of microsporidia spore adherence and host cell infection by the divalent cations (Southern and others 2006).

Like many other pathogenic intracellular organisms, microsporidia appear to use adherence to the host cell surface as a mechanism to facilitate infection. To identify microsporidia proteins potentially involved in adherence, the *E. cuniculi* genome database was searched for genes that encode proteins with recognizable adhesion domains. A protein (CAD25398) with sequence homology to members of the ADAM (a disintegrin and metalloprotease domain) family was found during this search. ADAMs are a group of type I transmembrane glycoproteins involved in a variety of biological processes including cell adhesion, proteolysis, cell fusion, and signaling (White 2003). Analysis of MADAM using the Conserved Domain Database revealed motifs in the sequence similar to those found in the

snake venom disintegrins (E-value = $4e^{-13}$) and zinc-dependent metalloproteases (E-value = $1e^{-5}$), which includes the ADAM family (Marchler-Bauer and Bryant 2004).

Most ADAMs share a common multi-domain organization consisting of a signal sequence, a pro-domain, a metalloprotease domain, a disintegrin-like domain, a cysteine-rich domain, an epidermal growth factor (EGF)-like domain, and a transmembrane domain followed by a cytoplasmic tail (White 2003). MADAM has a predicted signal sequence, pro-domain, metalloprotease domain, disintegrin-like domain, and a transmembrane domain but lacks a recognizable cysteine-rich domain, EGF-like domain, and cytoplasmic tail. In addition, MADAM contains a region of unknown homology located between the disintegrin and transmembrane domains. Based on global pairwise alignment, MADAM appears to possess a conserved zinc-dependent catalytic site (HExxHxxGxxH) and 'Met-Turn'. Therefore, MADAM is predicted to be catalytically active. Global pairwise alignment of the MADAM disintegrin domain with other ADAMs demonstrates that sequence identities range from 33% for ADAM10 to 41% for ADAM9. MADAM shares a high level of identity with other ADAMs due in part to the presence of fourteen conserved cysteine residues within its disintegrin domain. MADAM also contains a five amino acid insertion (NIHKM) within the area considered to be the integrin-binding region of the disintegrin domain. The significance of this amino acid insertion within the integrin-binding region remains to be determined.

Consequently, the characterization of MADAM was obviously important because of its potential involvement in processes such as cell adhesion, proteolysis, cell fusion, and signaling. Also, characterization of MADAM could provide the field of ADAM research with a unique representative from a fungal pathogen. Our examination of MADAM was divided into three objectives. First, we sought to determine the location of MADAM within the microsporidia spore. Identification of MADAM on the spore surface or in the polar tube

would suggest that MADAM could facilitate events such as spore adherence or polar tube extrusion. Second, we used an already established *in vitro* system to assay if MADAM is involved in spore adherence to the host cell and/or host cell infection. Third, was the identification of potential substrates or binding partners for MADAM using yeast two-hybrid. By completing these objectives, we were able to provide an initial characterization of MADAM the protein.

Immunoelectron microscopy was performed on *E. cuniculi* and *E. intestinalis* infected host cells using antibodies generated against the rMADAM-His-Tag protein. Our data demonstrate that MADAM is localized to the polar sac-anchoring disk complex of mature *E. cuniculi* and *E. intestinalis* spores. The polar sac-anchoring disk complex serves as an anchor between the polar tube and spore wall during polar tube extrusion. In addition to being localized to the polar sac-anchoring disk complex, MADAM can be found in the exospore and plasma membrane of *E. intestinalis* spores. In *E. cuniculi*, MADAM is only localized to the polar sac-anchoring disk complex. The exospore is the electron-dense, surface exposed layer of the microsporidia spore wall (Wittner 1999). In the spore wall, the plasma membrane lines the internal surface of the endospore (Wittner 1999). A difference in MADAM localization between *E. cuniculi* and *E. intestinalis* was unexpected. Originally *E. intestinalis* was classified as *Septata intestinalis* but was reclassified to the genus *Encephalitozoon* based on genetic and immunological studies (Hartskeerl and others 1995). The amount of sequence homology between MADAM from *E. cuniculi* and MADAM from *E. intestinalis* is not known because the sequence for the *E. intestinalis* protein has not been determined. MADAM does not represent the first protein to demonstrate variation among the species within the genus *Encephalitozoon*. For example, spore wall protein 1 (SWP1) and spore wall protein 2 (SWP2) are both expressed in *E. intestinalis* but only SWP1 is

expressed in *E. cuniculi* and *E. hellem* (Hayman and others 2001). Our demonstration that the expression pattern of MADAM differs between *E. cuniculi* and *E. intestinalis* may support the argument that *E. intestinalis* is unique within the genus (Hayman and others 2001).

Closer examination of the immunoelectron microscopy data demonstrated that MADAM protein expression is developmentally or differentially regulated in *E. intestinalis*. Early during the process of merogony, MADAM expression occurs internally and on the periphery but continues to become more intense and delineated as the spores develop. In some spores, MADAM expression occurs on the plasma membrane while in other spores expression occurs on the exospore. Expression appears to be limited to one or the other location and rarely does MADAM localize to both the exospore and plasma membrane within the same spore.

Localization of MADAM to different structures within *E. intestinalis* spores may be an indication of spore maturity. Exospore localization occurs on spores that are forming an electron dense outer exospore layer. Localization of MADAM to the plasma membrane appears to occur in spores without this electron dense exospore layer. Alternatively, localization of MADAM to the exospore or plasma membrane may indicate differences in protein maturity. MADAM localized to the plasma membrane may still possess the pro-domain while localization to the exospore may indicate loss of the pro-domain and maturation of the MADAM protein. Unfortunately, our attempt to generate antibodies specific for the MADAM pro-domain alone or the MADAM metalloprotease domain alone were unsuccessful. The significance of MADAM protein expression patterns within *E. intestinalis* will be difficult to examine without the availability of a suitable system to genetically manipulate the microsporidia.

Localization of MADAM to the surface exposed exospore and within the polar sac-anchoring disk complex of *E. intestinalis* indicates that MADAM could potentially be involved in adherence of the spore to the host cell and/or polar tube extrusion. A series of *in vitro* assays were performed to determine if the rMADAM-His-Tag protein could be used to manipulate microsporidia spore adherence and/or host cell infection. rMADAM-His-Tag protein was unable to significantly inhibit *E. cuniculi* spore adherence to the host cell monolayer. This observation was not unexpected given that MADAM was not localized to the exospore of *E. cuniculi*. rMADAM-His-Tag protein was able to decrease the occurrence of *E. intestinalis* spore adherence to the host cell monolayer by 50%-80%. Addition of the rMET-His-Tag or the rPRO-His-Tag protein to the spore adherence assay did not result in significant inhibition of *E. intestinalis* spore adherence. This information indirectly indicates that the MADAM disintegrin domain may be involved in the process of spore adherence. Attempts to recombinantly express the MADAM disintegrin domain alone for use in spore adherence assays were unsuccessful.

Surprisingly, host cell infectivity assays revealed that the rMADAM-His-Tag protein was only able to decrease the occurrence of host cell infection by less than 20%. This observation was unexpected given that the rMADAM-His-Tag protein decreased *E. intestinalis* spore adherence by 50%-80%. As a control, spore adherence and host cell infectivity assays using CSA were included. Addition of exogenous CSA resulted in at least a 40% decrease in *E. intestinalis* spore adherence and host cell infection. We currently do not have an alternative method to examine and manipulate the process of spore adherence. If a genetics system was available for microsporidia, we could suppress the expression of MADAM then examine the ability of the spores to adhere to the host cell surface and infect

the host cell. Considering our current data, we cannot conclusively state that MADAM is involved in the process of spore adherence or host cell infection.

As a protein sharing sequence homology with members of the ADAM family, it is possible that the MADAM protein has several functions. To better understand what role MADAM serves, it is necessary to identify potential substrates or binding partners. MADAM has the potential to interact with numerous host cell and/or microsporidia proteins. A yeast two-hybrid approach was used to identify such protein-protein interactions involving MADAM.

After evaluating the yeast two-hybrid data, we found *E. intestinalis* methionine aminopeptidase 2 (MetAP2) and *E. intestinalis* polar tube protein 3 (PTP3) to be the most interesting potential partners for the MADAM protein. MetAP2 is an essential participant in the N-terminal methionine excision pathway and is responsible for post-translational modification of nascent proteins by removing the N-terminal methionine (Upadhyya and others 2006). Fumagillin, one of the therapies used for the treatment of human microsporidiosis, covalently binds to MetAP2 and specifically inhibits the peptidase activity. Although the potential interaction between MetAP2 and MADAM is worth characterizing further, we were more interested in investigating PTP3 protein for several reasons. First, the PTP3 cDNA insert was positively identified from sequencing data from three separate colonies and several other colonies possessed cDNA inserts of the same size as the positively identified PTP3 cDNA inserts. We assumed that these colonies also contain a PTP3 cDNA insert. In addition, a potential interaction between MADAM and PTP3 seemed possible given that MADAM was localized to the polar sac-anchoring disk complex.

In situ analysis reveals that PTP3 is a slightly acidic protein (pI 6.47) of ~136kDa with a large acidic core flanked by highly basic N- and C-terminal domains (Peuvel and others 2002). Addition of a cross-linking reagent to crude extracts of *E. cuniculi* spores led to the

formation of a large protein complex consisting of five major proteins (Peuvel and others 2002). PTP1 and PTP2 were the predominant components of the complex while the slowest migrating band was representative of PTP3 (Peuvel and others 2002). PTP3 lacks cysteine residues but is rich in charged residues and it has been suggested that PTP3 may interact with PTP1 and/or PTP2 via ionic bonds to aid in the formation of PTP1-PTP2 polymers during polar tube extrusion (Peuvel and others 2002). The two other proteins within the complex located at ~75kDa and ~28kDa remain to be identified. In order to determine if the ~75kDa protein within the protein complex was MADAM, we attempted to duplicate the cross-linking experiment but were unsuccessful (data not shown).

To further characterize the potential interaction between MADAM and PTP3, additional yeast two-hybrid experiments were performed. First, we evaluated *E. cuniculi* PTP3 for an interaction with MADAM. Our yeast two-hybrid experiments indicated that MADAM has the ability to interact with PTP3 from *E. cuniculi* and *E. intestinalis*. To more specifically identify which MADAM domain or domains were responsible for the potential interaction with PTP3, several MADAM deletion mutants were generated and evaluated. Deletion of the unknown region alone or in combination with the disintegrin domain did not appear to decrease the interaction between MADAM and EiPTP3. However, deletion of the disintegrin domain in combination with the unknown region did appear to slightly decrease the ability of MADAM to interact with EcPTP3. The ability of MADAM to interact with EcPTP3 and EiPTP3 was almost completely eliminated upon removal of the metalloprotease domain. Our yeast two-hybrid analyses at least indirectly indicate that the interaction between MADAM and PTP3 relies on the MADAM metalloprotease domain. Further yeast two-hybrid experiments should be conducted using a MADAM construct that consists of a mutated metalloprotease catalytic site instead of a complete deletion of the metalloprotease domain.

Yeast two-hybrid screens were also performed to determine if MADAM interacts with either PTP1 or PTP2. According to our yeast two-hybrid data, MADAM appears to interact with both EcPTP1 and EcPTP2 but does not interact with EcPTP2 as strongly as it does with EcPTP1 or EcPTP3. Interestingly, MADAM does not interact with EiPTP1 as strongly as it does with EiPTP2 or EiPTP3. PTP1 is a proline-rich acidic protein with a highly variable repeat-containing core while PTP2 is a lysine-rich basic protein with an acidic tail. EcPTP1 and EiPTP1 share 80% identity while EcPTP2 and EiPTP2 only share 49% homology. Again, identification of different interactions involving MADAM from *E. cuniculi* versus *E. intestinalis* could be attributed to *E. intestinalis* being unique within the *Encephalitozoon* genus. The interactions between EcPTP2-MADAM and EcPTP3-MADAM were confirmed by *in vitro* co-immunoprecipitation.

Future studies should include completion of our yeast two-hybrid screening and additional confirmation of potential protein interactions. A major obstacle facing the characterization of interactions involving the MADAM protein is the lack of *in vivo* methods. As stated previously, a system to genetically manipulate microsporidia does not exist. In addition, the examination of interactions involving native microsporidia proteins is challenging given that the proteins are most often isolated in the presence of high concentrations of an ionic detergent and reducing agent.

Overall, our research has established a foundation for further characterization of the MADAM protein. We demonstrated the location of MADAM within *E. cuniculi* and *E. intestinalis* spores. We established that yeast two-hybrid analysis is a method suitable for the field of microsporidia research. Finally, our preliminary yeast two-hybrid analyses indicate that MADAM may provide some function during polar tube extrusion through an

interaction involving the MADAM metalloprotease domain and components of the polar tube, specifically PTP3.

REFERENCES

- Aebersold R, Mann M. 2003. Mass spectrometry-based proteomics. *Nature* 422(6928):198-207.
- Altschul SF, Gish W, Miller W, Myers EW, Lipman DJ. 1990. Basic local alignment search tool. *J Mol Biol* 215(3):403-10.
- Anzinger JJ, Mezo I, Ji X, Gabali AM, Thomas LL, Spear GT. 2006. HIV infection of mononuclear cells is calcium-dependent. *Virus Res* 122(1-2):183-8.
- Bigliardi E, Sacchi L. 2001. Cell biology and invasion of the microsporidia. *Microbes Infect* 3(5):373-9.
- Causier B, Davies B. 2002. Analysing protein-protein interactions with the yeast two-hybrid system. *Plant Mol Biol* 50(6):855-70.
- Clontech. 2006 Mar 16. Matchmaker™ Co-IP Kit User Manual. <<http://www.clontech.com>>. Accessed 2007 Jun 10.
- Clontech. 2007 Apr 20. Matchmaker™ Construction & Screening Kits User Manual. <<http://www.clontech.com>>. Accessed 2007 Jun 10.
- Conteas CN, Berlin OG, Ash LR, Pruthi JS. 2000. Therapy for human gastrointestinal microsporidiosis. *Am J Trop Med Hyg* 63(3-4):121-7.
- Croppo GP, Croppo GP, Moura H, Da Silva AJ, Leitch GJ, Moss DM, Wallace S, Slemenda SB, Pieniazek NJ, Visvesvara GS. 1998. Ultrastructure, immunofluorescence, western blot, and PCR analysis of eight isolates of *Encephalitozoon (Septata) intestinalis* established in culture from sputum and urine samples and duodenal aspirates of five patients with AIDS. *J Clin Microbiol* 36(5):1201-8.
- del Aguila C, Izquierdo F, Granja AG, Hurtado C, Fenoy S, Fresno M, Revilla Y. 2006. *Encephalitozoon* microsporidia modulates p53-mediated apoptosis in infected cells. *Int J Parasitol* 36(8):869-76.

- Deplazes P, Mathis A, Weber R. 2000. Epidemiology and zoonotic aspects of microsporidia of mammals and birds. *Contrib Microbiol* 6:236-60.
- Didier ES, Stovall ME, Green LC, Brindley PJ, Sestak K, Didier PJ. 2004. Epidemiology of microsporidiosis: sources and modes of transmission. *Vet Parasitol* 126(1-2):145-66.
- Didier ES, Weiss LM. 2006. Microsporidiosis: current status. *Curr Opin Infect Dis* 19(5):485-92.
- Eto K, Huet C, Tarui T, Kupriyanov S, Liu HZ, Puzon-McLaughlin W, Zhang XP, Sheppard D, Engvall E, Takada Y. 2002. Functional classification of ADAMs based on a conserved motif for binding to integrin alpha 9beta 1: implications for sperm-egg binding and other cell interactions. *J Biol Chem* 277(20):17804-10.
- Gasteiger E, Gattiker A, Hoogland C, Ivanyi I, Appel RD, Bairoch A. 2003. ExPASy: The proteomics server for in-depth protein knowledge and analysis. *Nucleic Acids Res* 31(13):3784-8.
- Hallak LK, Spillmann D, Collins PL, Peebles ME. 2000. Glycosaminoglycan sulfation requirements for respiratory syncytial virus infection. *J Virol* 74(22):10508-13.
- Hartskeerl RA, Van Gool T, Schuitema AR, Didier ES, Terpstra WJ. 1995. Genetic and immunological characterization of the microsporidian *Septata intestinalis* Cali, Kotler and Orenstein, 1993: reclassification to *Encephalitozoon intestinalis*. *Parasitology* 110 (Pt 3):277-85.
- Hayman JR, Hayes SF, Amon J, Nash TE. 2001. Developmental expression of two spore wall proteins during maturation of the microsporidian *Encephalitozoon intestinalis*. *Infect Immun* 69(11):7057-66.
- Hayman JR, Nash TE. 1999. Isolating expressed microsporidial genes using a cDNA subtractive hybridization approach. *J Eukaryot Microbiol* 46(5):21S-24S.
- Hayman JR, Southern TR, Nash TE. 2005. Role of sulfated glycans in adherence of the microsporidian *Encephalitozoon intestinalis* to host cells *in vitro*. *Infect Immun* 73(2):841-8.

- Huxley-Jones J, Clarke TK, Beck C, Toubaris G, Robertson DL, Boot-Handford RP. 2007. The evolution of the vertebrate metzincins; insights from *Ciona intestinalis* and *Danio rerio*. *BMC Evol Biol* 7:63.
- Leitch GJ, Ward TL, Shaw AP, Newman G. 2005. Apical spore phagocytosis is not a significant route of infection of differentiated enterocytes by *Encephalitozoon intestinalis*. *Infect Immun* 73(11):7697-704.
- Maple J, Moller SG. 2007. Yeast two-hybrid screening. *Methods Mol Biol* 362:207-23.
- Marchler-Bauer A, Bryant SH. 2004. CD-Search: protein domain annotations on the fly. *Nucleic Acids Res* 32(Web Server issue):W327-31.
- Mathis A, Weber R, Deplazes P. 2005. Zoonotic potential of the microsporidia. *Clin Microbiol Rev* 18(3):423-45.
- Peuvel I, Peyret P, Metenier G, Vivares CP, Delbac F. 2002. The microsporidian polar tube: evidence for a third polar tube protein (PTP3) in *Encephalitozoon cuniculi*. *Mol Biochem Parasitol* 122(1):69-80.
- Reiss K, Ludwig A, Saftig P. 2006. Breaking up the tie: disintegrin-like metalloproteinases as regulators of cell migration in inflammation and invasion. *Pharmacol Ther* 111(3):985-1006.
- Rise M, Burke RD. 2002. SpADAM, a sea urchin ADAM, has conserved structure and expression. *Mech Dev* 117(1-2):275-81.
- Rostand KS, Esko JD. 1997. Microbial adherence to and invasion through proteoglycans. *Infect Immun* 65(1):1-8.
- Scanlon M, Shaw AP, Zhou CJ, Visvesvara GS, Leitch GJ. 2000. Infection by microsporidia disrupts the host cell cycle. *J Eukaryot Microbiol* 47(6):525-31.
- Seals DF, Courtneidge SA. 2003. The ADAMs family of metalloproteases: multidomain proteins with multiple functions. *Genes Dev* 17(1):7-30.
- Southern TR, Jolly CE, Russell Hayman J. 2006. Augmentation of microsporidia adherence and host cell infection by divalent cations. *FEMS Microbiol Lett* 260(2):143-9.

- Stocker W, Grams F, Baumann U, Reinemer P, Gomis-Ruth FX, McKay DB, Bode W. 1995. The metzincins—topological and sequential relations between the astacins, adamalysins, serralysins, and matrixins (collagenases) define a superfamily of zinc-peptidases. *Protein Sci* 4(5):823-40.
- Tousseyn T, Jorissen E, Reiss K, Hartmann D. 2006. (Make) stick and cut loose—disintegrin metalloproteases in development and disease. *Birth Defects Res C Embryo Today* 78(1):24-46.
- Upadhy R, Zhang HS, Weiss LM. 2006. System for expression of microsporidian methionine amino peptidase type 2 (MetAP2) in the yeast *Saccharomyces cerevisiae*. *Antimicrob Agents Chemother* 50(10):3389-95.
- Vidalain PO, Boxem M, Ge H, Li S, Vidal M. 2004. Increasing specificity in high-throughput yeast two-hybrid experiments. *Methods* 32(4):363-70.
- Vivares CP, Metenier G. 2001. The microsporidian *Encephalitozoon*. *Bioessays* 23(2):194-202.
- White JM. 2003. ADAMs: modulators of cell-cell and cell-matrix interactions. *Curr Opin Cell Biol* 15(5):598-606.
- Wittner M. 1999. *The Microsporidia and Microsporidiosis*. Washington, DC: American Society for Microbiology.
- Xu Y, Weiss LM. 2005. The microsporidian polar tube: a highly specialised invasion organelle. *Int J Parasitol* 35(9):941-53.
- Zhu YY, Machleder EM, Chenchik A, Li R, Siebert PD. 2001. Reverse transcriptase template switching: a SMART approach for full-length cDNA library construction. *Biotechniques* 30(4):892-7.

VITA

CARRIE E. JOLLY

Personal Data:

Date of Birth: February 1, 1979
Place of Birth: Statesville, North Carolina
Marital Status: Married

Education:

Ph.D. Biomedical Sciences, East Tennessee State University, Johnson City, Tennessee 2007
B.S. Biology, East Tennessee State University, Johnson City, Tennessee 2002

Professional Experience:

Graduate Assistant, East Tennessee State University, Quillen College of Medicine, 2002–2007

Publications:

Southern, T.R., Jolly, C.E., Lester, M.E., Hayman, J.R. (2007) EnP1, a microsporidia spore wall protein that enables spores to adhere and infect host cells *in vitro*. *Eukaryot Cell*. 6(8):1354-62

Southern, T.R., Jolly, C.E., Lester, M.E., Hayman, J.R. (2006) Identification of a Microsporidia Protein Potentially Involved in Spore Adherence to Host Cells. *J. Eukaryot. Microbiol.* 53(S1):S68-S69.

Southern, T.R., Jolly, C.E., Hayman, J.R. (2006) Augmentation of Microsporidia Adherence and Host Cell Infection by Divalent Cations. *FEMS Microbiology Letters*. 260: 143-149.

Worsham, L.M., Earls, L., Jolly, C., Langston, K.G., Trent, M.S., Ernst-Fonberg, M.L. (2003) Amino Acid Residues of *Escherichia coli* Acyl Carrier Protein Involved in Heterologous Protein Interactions. *Biochemistry*. 42(1):167-76.

Worsham, L.M., Trent, M.S., Earls, L., Jolly, C., Ernst-Fonberg, M.L. (2001) Insights into the Catalytic Mechanism of HlyC, the Internal Protein Acyltransferase that Activated Amino *Escherichia coli* Hemolysin Toxin. *Biochemistry*. 40(45):13607-16.

Honors and Awards:

Appalachian Student Research Forum Post-Baccalaureate Oral Presentation-Second Place, 2007

James H. Quillen Scholarship, 2005

American Society for Microbiology Corporate Activities Program Student Travel Grant, 2004